[CANCER RESEARCH 57, 4285–4300, October 1, 1997]

Characterization of the *p53* Tumor Suppressor Pathway in Cell Lines of the National Cancer Institute Anticancer Drug Screen and Correlations with the Growth-Inhibitory Potency of 123 Anticancer Agents

Patrick M. O'Connor,[1] Joany Jackman, Insoo Bae, Timothy G. Myers, Saijun Fan, Masato Mutoh, Dominic A. Scudiero, Ann Monks, Edward A. Sausville, John N. Weinstein, Stephen Friend, Albert J. Fornace, Jr., and Kurt W. Kohn

Laboratory of Molecular Pharmacology, Division of Basic Sciences, National Cancer Institute, NIH, Bethesda, Maryland 20892 [P. M. O., J. J., I. B., T. G. M., S. Fa., M. M., J. N. W., A. J. F., K. W. K.]; Developmental Therapeutics Program, National Cancer Institute, Frederick Cancer Research & Development Center, Frederick, Maryland 21702 [D. A. S., A. M., E. A. S.]; and Laboratory of Molecular Pharmacology, Fred Hutchinson Cancer Center, Seattle, Washington 98104 [S. Fr.]

ABSTRACT

In the present study, we report the characterization of the *p53* tumor suppressor pathway in the 60 cell lines of the National Cancer Institute (NCI) anticancer drug screen, as well as correlations between the integrity of this pathway and the growth-inhibitory potency of 123 anticancer agents in this screen. Assessment of *p53* status in these lines was achieved through complete *p53* cDNA sequencing, measurement of basal p53 protein levels and functional assessment of (*a*) transcriptional activity of *p53* cDNA from each line in a yeast assay, (*b*) γ-ray-induced G_1 phase cell cycle arrest, and (*c*) γ-ray-induced expression of *CIP1/WAF1*, *GADD45*, and *MDM2* mRNA. Our investigations revealed that *p53* gene mutations were common in the NCI cell screen lines: 39 of 58 cell lines analyzed contained a mutant *p53* sequence. cDNA derived from almost all of the mutant *p53* cell lines failed to transcriptionally activate a reporter gene in yeast, and the majority of mutant *p53* lines studied expressed elevated basal levels of the mutant p53 protein. In contrast to most of the wild-type *p53*-containing lines, cells containing mutant *p53* sequence were also deficient in γ-ray induction of *CIP1/WAF1*, *GADD45*, and *MDM2* mRNA and the ability to arrest in G_1 following γ-irradiation. Taken together, these assessments provided indications of the integrity of the *p53* pathway in the 60 cell lines of the NCI cell screen. These individual *p53* assessments were subsequently used to probe a database of growth-inhibitory potency for 123 "standard agents," which included the majority of clinically approved anticancer drugs. These 123 agents have been tested against these lines on multiple occasions, and a proposed mechanism of drug action had previously been assigned to each agent. Our analysis revealed that cells with mutant *p53* sequence tended to exhibit less growth inhibition in this screen than the wild-type *p53* cell lines when treated with the majority of clinically used anticancer agents: including DNA cross-linking agents, antimetabolites, and topoisomerase I and II inhibitors. Similar correlations were uncovered when we probed this database using most of the other indices of *p53* status we assessed in the lines. Interestingly, a class of agents that differed in this respect was the antimitotic agents. Growth-inhibitory activity of these agents tended, in this assay, to be independent of *p53* status. Our characterization of the *p53* pathway in the NCI cell screen lines should prove useful to researchers investigating fundamental aspects of *p53* biology and pharmacology. This information also allows for the large-scale analysis of the more than 60,000 compounds tested against these lines for novel agents that might exploit defective *p53* function as a means of preferential toxicity.

Received 4/25/97; accepted 7/25/97.

The costs of publication of this article were defrayed in part by the payment of page charges. This article must therefore be hereby marked *advertisement* in accordance with 18 U.S.C. Section 1734 solely to indicate this fact.

[1] To whom requests for reprints should be addressed, at Laboratory of Molecular Pharmacology, Division of Basic Science, Building 37, Room 5C25, National Cancer Institute, NIH, Bethesda, MD 20892. Phone: (301) 435-2848; Fax: (301) 402-0752; E-mail: oconnorp@dc37a.nci.nih.gov.

INTRODUCTION

The Developmental Therapeutics Program of the NCI[2] uses 60 human cell lines derived from cancers of the colon, breast, ovary, lung, kidney, central nervous system, skin, and bone marrow as a screen to discover novel anticancer agents (1–3). The chemical repository from which compounds are taken for analysis consists of approximately 300,000 agents and is growing. Such agents are submitted for testing from a wide variety of sources, including individual investigators, biotechnology, and pharmaceutical companies; the agents are not limited to synthetic agents but include natural products. Approximately 60,000 agents have presently been tested in the NCI anticancer drug screen, and the rate of testing averages approximately 10,000 compounds per year. Of these 60,000 agents, approximately 8,000 have been considered for analysis in additional *in vitro* and *in vivo* assay systems, including studies in a panel of human tumor xenografts established in nude mice (1–4). To date, five drugs (UCN-01, flavopyridol, the spicamycin analogue KRN 5500, a quinocarmycin analogue, and a depsipeptide) have been selected for Phase I clinical evaluation based in part on activity in the NCI anticancer drug screen.

The NCI anticancer drug screen evaluates the growth-inhibitory effects of a compound in 60 cancer cell lines. Growth inhibition is measured in a 96-microwell format on the basis of cellular protein content (1–3). The growth fraction relative to a vehicle control is measured 48 h after the introduction of the compound at each of five concentrations covering a 4-log dose range. The dose-response curves are used to determine the GI_{50}. Reducing each experiment to an array of 60 GI_{50}s results in a pattern of activity for each tested compound. These activity patterns, also called "fingerprints," have been exploited using display techniques such as the "mean graph" (1–3); the COMPARE algorithm, which searches among the database of tested compounds for agents with similar activity patterns (5–7); and the DISCOVERY program package, which incorporates additional analytical applications (8, 9). Taken together, the COMPARE and DISCOVERY programs have proven useful in classifying unknown compounds as topoisomerase inhibitors, antimitotics, or pyrimidine biosynthesis inhibitors (5–8, 10).

The 60 cell lines in the NCI anticancer drug screen are presently undergoing extensive molecular characterization to better define them in terms of the status of tumor suppressor genes, oncogenes, enzymes, and/or biological processes commonly altered in human cancer. This molecular search aims to uncover the basis of the differential chemosensitivity responses of the lines in the screen and may ultimately shape new approaches to the discovery of "lead compounds" with preferential activity toward cancer cells with defined molecular de-

[2] The abbreviations used are: NCI, National Cancer Institute; GI_{50}, dose of agent required to inhibit growth of the cells by 50% of the vehicle control sample following a 48-h continuous exposure.

fects. Detailed knowledge of the molecular characteristics of these cell lines might also uncover interrelationships between individual components or pathways. Published examples of recent molecular dissection efforts in the NCI cell screen lines that have in turn uncovered chemosensitivity relationships include the analysis of P-glycoprotein and, recently, the *ras* oncogene (11–15).

In the present study, we report the status of the *p53* tumor suppressor pathway in the 60 cell lines of the NCI anticancer drug screen. Our interest in the characterization of the *p53* pathway in these cell lines was stimulated by (*a*) the high frequency with which *p53* is altered in human tumors (16–18), and (*b*) the fact that we and others have found that *p53* dysfunction can in some instances alter sensitivity to ionizing radiation and at least some chemotherapeutic drugs (19–27). The goals of our study were to (*a*) provide a detailed picture of the status of the *p53* pathway in these cell lines and (*b*) to use this knowledge to uncover the impact of *p53* status on the growth-inhibitory activity of a set of 123 "standard agents" that included most of the clinical agents approved for cancer treatment. These 123 agents have been tested in this primary screen on multiple occasions and have been assigned putative mechanisms of action (5, 8, 10).

Our assessment of *p53* status in the NCI screen lines revealed that *p53* mutations were common and that the majority of these mutant *p53* cell lines lacked *p53*-dependent transactivation function as well as the ability to arrest in G_1 following γ-irradiation. Also, in contrast to almost all of the wild-type *p53* cell lines studied, the majority of the mutant *p53* lines exhibited elevated basal levels of the mutant p53 protein. By using these assessments to investigate the growth-inhibitory activity of 123 standard agents of putatively known mechanism of action (5, 8, 10), we found that the mutant *p53* cell lines tended, on average, to be less sensitive than the wild-type *p53* lines to the majority of alkylating agents, DNA/RNA antimetabolites, and topoisomerase I and II inhibitors tested in this assay. A class of agents that differed in this respect, however, was the set of antimitotic agents, including paclitaxel and vincristine. Our results suggest that for the majority of agents within the antimitotic class, *p53* status was not an indicator of growth-inhibitory activity in the NCI screening assay.

MATERIALS AND METHODS

Cell Lines and *in Vitro* Chemosensitivity Testing. The collection and basic characterization of the 60 cell lines in the NCI anticancer drug screen has been extensively described (1–3). All cell lines were grown in RPMI 1640 that contained 5% fetal bovine serum with 5 mM L-glutamine, and cells were routinely replaced in culture every 20 passages with samples from cryopreserved stocks. Compounds were screened for their effect on cell growth using a 48-h assay with sulforhodamine B assay essentially as described previously (1–3). The measure of chemosensitivity referred to in this report is the GI_{50} value. Each agent was tested in 2–460 independent experiments (median, 5 experiments). All 60 cell lines were assayed in parallel for each agent evaluated, and routine quality control criteria were used to exclude unsatisfactory dose-response curves (1–3, 5).

Statistical Analysis. Because *p53* mutation status is a binary parameter and other *p53*-associated characteristics could reasonably be rendered as binary, and because the GI_{50} measurements for each drug do not all follow a normal distribution, we chose the Wilcoxon (Kruskal-Wallis) rank sum test (normal approximation) to measure the strength of the association between these binary parameters and the GI_{50} activity values. High levels of an individual characteristic (*e.g.*, high basal p53 protein levels) were coded as 1 and low values as 0, thus dividing the lines into two groups with respect to that characteristic. In the case of *p53* mutation status, wild-type cell lines were coded as 1 and mutant cell lines as 0. The one heterozygote (HCT-15) was coded as 0 for consistency with the expected dominant-negative effect of the mutant p53 protein. The threshold value for each of the other characteristics measured is given in the legend of Fig. 8.

A program for doing large numbers of Wilcoxon rank sum calculations (normal approximation) was written by SAS (SAS Institute, Cary, NC) for these analyses. The Wilcoxon rank sum test provides a nonparametric test of the null hypothesis that for any given characteristic, the cells coded as 0 have the same sensitivity to an agent as do the cells coded as 1. For the Wilcoxon p value (range, 0–1), a number less than 0.5 indicates a tendency for the mutant cells to be more sensitive than the wild-type cells; a number greater than 0.5 indicates the opposite. Formally, a p value less than 0.025 or greater than 0.975 is required to reject the null hypothesis of equal median sensitivities at the 5% level of confidence (two-sided). However, because the 60 cell lines do not represent a random sample selected from an assumed underlying population, the p value as used here should be thought of as a heuristic parameter indicating tendency, rather than as a formal statistical entity.

***p53* cDNA Sequencing.** Polyadenylated mRNA was extracted from cells using a MicroFast Track mRNA isolation kit (Invitrogen) and cDNA prepared using a First-Strand cDNA synthesis kit (Pharmacia) according to the manufacturers' recommendations. Three overlapping *p53*-specific PCR primers covering the entire open reading frame were used to bidirectionally sequence the *p53* cDNA using Taq dideoxy sequencing methodology on an Applied Biosystems model 373A automated sequencer (Applied Biosystems; Ref. 28).

Functional Analysis of *p53* cDNA in Yeast. Functional analysis of separated *p53* alleles in yeast (FASAY) was performed essentially as described previously (28). Briefly, the FASAY assay measures the transcriptional activity of *p53* cDNA from the individual cell lines in a yeast survival assay. The assay uses three centromeric plasmids. The first plasmid, pLS76 (positive control), contains a LEU2 gene for selection of transformed yeast on plates lacking leucine, and full-length wild-type human *p53* cDNA expressed under the control of the ADH1 promoter. The second plasmid, pSS16, is identical to pLS76 except that the wild-type *p53* sequence from codons 68–347 is replaced by the URA3 gene, which confers growth on plates lacking uracil. The third plasmid, pSS1, contains a HIS3 gene under the control of a single *p53* binding site derived from the ribosomal gene cluster (29). Input *p53* was generated from polyadenylated mRNA extracted from cells using a MicroFast Track mRNA isolation kit (Invitrogen) and cDNA prepared using a First-Strand cDNA synthesis kit (Pharmacia). *p53* cDNA was PCR amplified using Pfu polymerase (Stratagene), and yeast was cotransfected with the PCR-generated *p53* and *Hin*dIII/*Stu*I-restricted plasmid pSS16 (which releases the URA3 gene segment). Repair of the gapped pSS16 plasmid with the *p53* derived from the input *p53* PCR product occurs *in vivo* through homologous recombination. Transformants that have successfully repaired pSS16 are selected on media lacking leucine, and such replicates lack growth on uracil-minus media. If the yeast has also been transfected with pSS1, then growth on media lacking histidine identifies colonies that contain transcriptionally active *p53*. Leu^+ colonies containing only wild-type *p53* sequences grew successfully on plates lacking histidine. Leu^+ colonies containing only *p53* "loss-of-function" mutations failed to grow on plates lacking histidine. Leu^+ colonies derived from *p53* cDNA prepared from cancer cells containing heterozygous *p53* gene status yield approximately 50% His^+ colonies (28).

Gel Electrophoresis and Western Blotting. Protein isolation and analysis were performed essentially as described (20). Briefly, cells were lysed on ice for 30 min in 1% NP-40 prepared in PBS that contained 10 μg/ml leupeptin, 10 μg/ml aprotinin, 2 mM 4-(2-aminoethyl)-benzenesulfonyl fluoride, 1 mM sodium orthovanadate, 10 mM sodium fluoride, and 5 mM sodium PP_i. Protein determination was performed using the BCA protein assay kit according to the manufacturer's instructions (Pierce). One hundred μg of total cell protein were loaded onto SDS-polyacrylamide gels, and then proteins were transferred to Immobilon membranes (Millipore) using semidry blotting techniques. Membranes were blocked for 30 min in 5% skim milk, probed for 1 h with the mouse monoclonal p53 primary antibody, Pab 1801, which recognizes an epitope that resides between amino acids 32 and 79 of p53 (Oncogene Science), and then probed with a sheep antimouse horseradish peroxidase second antibody (Amersham Corp.). Antibody reaction was revealed using chemiluminescence detection according to the manufacturer's recommendations (Amersham Corp.). Proliferating cell nuclear antigen was probed for as an additional control for gel loadings and was found not to vary by more than 25% between the different blots analyzed (data not shown). Comparisons between individual blots was accomplished by including 100 μg of total cell protein from the wild-type *p53* cell line, WMN, and the mutant *p53* cell line, CA46 (248 R/Q), on each blot (20, 21). The basal levels of p53 in each line were classified into two groups according to the level of p53 expression in WMN

cells (wild-type *p53*): low/negligible basal p53 levels (<2-fold that seen in WMN cells) and high basal p53 levels (≥2-fold that seen in WMN cells). High basal p53 levels were similar to those seen in the mutant *p53* line, CA46, which has previously been reported to express elevated levels of mutant p53 (20, 21).

Flow Cytometry. Twenty-four h prior to commencement of the G_1 arrest assay, plated cells were trypsinized and replated at 10–20% confluence. Twenty-four h later, floating cells were decanted from the plates, and fresh medium was added. For suspension cultures, exponentially growing cells were diluted to 5×10^5 cells/ml. Cells were irradiated at room temperature with 6.3 or 12.6 Gy of γ-rays using a ^{137}Cs source (5.25 Gy/min; 1 Gy = 100 rads) and then incubated for 17 h at 37°C in the presence or absence of the microtubule inhibitor nocodazole (0.1–0.4 μg/ml; Aldrich). Medium containing floating cells was combined with cells trypsinized from the plates and then centrifuged. Cells were then washed once in ice-cold PBS and fixed in 70% ethanol for a minimum of 2 h. Cells were rehydrated by being washed in PBS and then resuspended in propidium iodide (25 μg/ml; Sigma) that contained RNase A (500 units/ml; Sigma) before incubation at 37°C for 30 min. Cell cycle analysis was performed on a Becton Dickinson FACScan flow cytometer using the SOBR program provided by the manufacturer: 3–5 S-phase peaks were used to fit the model, and at least 15,000 cells were used for each analysis (Becton Dickinson). In some cases, nocodazole was included in the assay to prevent any cells that might break through the G_2 checkpoint from entering G_1 of the second cell cycle. Thus, the population of cells in G_1 17 h after incubation with nocodazole reflects cells in the first G_1 phase (20, 21). G_1 arrest was quantitated as the percentage of the control G_1 population that remained in G_1 17 h after irradiation plus incubation with nocodazole. G_1 arrest responses were grouped into three classes: class 1 cells showed strong G_1 arrest (>20% of the original G_1 population); class 2 cells showed intermediate G_1 arrest (between 10 and 20% of the original G_1 population); and class 3 cells showed weak or no G_1 arrest (<10% of original G_1 population).

RNA Isolation and Dot-Blot Hybridization. The induction of *WAF1/CIP1*, *GADD45*, and *MDM2* mRNA was assessed 4 h after exposure to 20 Gy of γ-rays essentially as described (30, 31). Briefly, exponentially growing and irradiated cells were lysed *in situ* using 4 M guanidine thiocyanate. Polyadenylated mRNA was prepared from total RNA using oligo(dT)-cellulose chromatography. Eight incremental 1:2 dilutions of the polyadenylated mRNA samples were blotted onto Nytran filters (Schleicher and Schuell) using a Hybri-dot manifold (Life Technologies, Inc., Gaithersburg, MD). Membranes were irradiated with UV light (700 J/m^2 at 254 nm). The first four dilutions were probed with either *CIP1/WAF1* (pZL-WAF-1), *GADD45* (pHulB2), or *MDM2* (FL4) cDNA ^{32}P-labeled probes. The *CIP1/WAF1* and *MDM2* probes were kindly provided by Dr. Bert Vogelstein (Johns Hopkins University, Baltimore, MD). The last four dilutions were hybridized with ^{35}S-labeled polythymidylate probe and also a ^{32}P-labeled probe to glyceraldehyde-3-phosphate dehydrogenase, which confirmed equivalent loadings between individual samples. The level of mRNA induction relative to unirradiated control samples for each transcript was grouped into three classes: class 1 cells showed strong mRNA induction (≥4-fold above basal levels); class 2 cells showed intermediate mRNA induction (between 2-fold and 4-fold); and class 3 cells showed weak or no mRNA induction (≤2-fold).

RESULTS

***p53* cDNA Sequencing.** *p53* sequencing was performed on cDNA prepared from polyadenylated mRNA extracted from each cell line. Three overlapping *p53*-specific primer pairs were used to bidirectionally sequence the entire *p53* cDNA using Taq polymerase with the aid of automated DNA sequencing procedures (see "Materials and Methods"). Of the 58 cell lines sequenced, 18 (31%) were found to contain wild-type *p53*, 39 (67%) contained only mutant *p53* sequence, and 1 (HCT-15) was heterozygous for *p53* mutation (Table 1). With the exception of the prostate lines, each tissue set contained at least one wild-type *p53* cell line (Table 1). The melanoma and renal cell line panels contained a higher proportion of wild-type *p53* lines [melanoma, 5 of 8 (63%); renal, 4 of 8 (50%)] compared to the remaining tissue sets (9 wild-type lines of 41 (28%): melanoma, p value = 0.033; renal, p value = 0.183; Fisher's exact test, two-tail).

The majority of *p53* mutations observed in the NCI screen lines were missense mutations [33 of 40 examples (83%)]; the most frequently observed missense mutations occurred at codons 248 (5 examples), 266 (4 examples), and 273 (5 examples; Fig. 1). Of the four lines with a codon 266 mutation (G/E), two were of the same origin: MDAMB435 and MDAN. These lines differ in that MDAN is a Her-2/neu-transfected derivative of MDAMB435 (32). Analysis of all *p53* mutations revealed a preponderance of G/A [17 of 41 (41.5%)] and G/T [5 of 41 (12%)] transitions (Table 2). Interestingly, one cell line harbored two base substitutions within the same codon (SK-MEL28: TGT/GTT), resulting in a change in a cysteine to a valine at amino acid position 145 (Table 1). Internal sequence deletions were also common [5 of 41 (12%)], whereas C/A and G/C transitions were relatively infrequent (Table 2). Also commonly observed among the 58 lines analyzed was a polymorphism at codon 72 [10 of 58 lines (24%); data not shown].

With only two exceptions, all of the *p53* mutations resided within the central evolutionarily conserved sequence-specific DNA binding domain of *p53* (Fig. 1; Ref. 33 and references therein). The two mutations seen outside this sequence-specific DNA binding domain were found at codon 309 (P/A transition) in the lung cancer cell line NCI-H226 and codon 336 (E to stop) in the renal cancer cell line SN12C (Table 1; Fig. 1). The codon 336 mutation would lead to a truncated p53 protein lacking most of the region required for *p53* oligomerization (amino acids 319–360), as well as a putative DNA damage recognition region (amino acids 311–393; Refs. 34 and 35).

Assay of *p53* cDNA Function in Yeast. The transcriptional activity of *p53* cDNA from each line was assessed in a yeast growth assay that selects for the *p53*-dependent expression of a survival gene that confers growth in the absence of histidine (Ref. 28; see "Materials and Methods"). Fifty-four of the 60 cell lines in the NCI screen were analyzed in this yeast growth assay. *p53* cDNA derived from 17 of these lines was capable of conferring growth in the absence of histidine. Fifteen of these lines contained wild-type *p53* sequence, whereas the other 2 lines (RPMI8226 and SKMEL2) contained mutations in *p53* (Table 1). *p53* cDNA derived from 36 lines failed to confer growth on media lacking histidine, and all of these lines contained mutant *p53*. These results supported the conclusion that these mutations were all loss-of-function mutations. *p53* in one of these lines, K562, was not sequenced in our studies; however, this line has been reported to contain mutant *p53* by other workers (18). *p53* cDNA derived from HCT15 cells yielded approximately half the number of yeast colonies compared to yeast transformed with only wild-type *p53* cDNA. This latter result was consistent with the heterozygous *p53* gene status of HCT15 cells (Table 1; Ref. 28). *p53* cDNA from two cell lines with mutations outside of the sequence-specific DNA binding domain of *p53* (SN12C, 336 E/stop, and NCIH226, 309 P/A) also failed to transcriptionally activate the *p53* reporter gene in yeast.

p53 Protein Levels and Relationship to *p53* Status. Basal levels of the p53 protein were determined from exponentially growing cells by means of Western blotting using the p53 mouse monoclonal antibody Pab1801. This antibody recognizes an epitope that resides between amino acids 32 and 79 of the p53 protein, and in Western blotting this antibody recognizes both wild-type and mutant p53 (20). Fig. 2 illustrates the results of our Western blot analysis on 55 of the cell lines in the NCI screen. In most cases, a single p53 band was observed by Western blotting. However, in some cells (*e.g.*, T47D, BT549, and OVCAR3) a second, faster-migrating band was also observed. Comparisons between individual blots was accomplished by including protein from the wild-type *p53* cell line WMN and the mutant *p53* cell line CA46 (248 R/Q) on each blot (20). The basal levels of p53 in each line were classified into two groups according to

Table 1 *p53 gene status in the cell lines of the NCI anticancer drug screen*

Cell line	Cancer type	p53 sequence codon change[a]	p53 sequence base change	p53 sequence amino acid change	Yeast assay[b]	Doubling time[c]	Cell cycle distribution[d]		
							% in G_1	% in S	% in G_2-M
MCF7	Breast	wt[e]		wt	wt	26	62.9	11.6	25.5
MCF7/ADR-RES		del 126–132		del 126–132	m	34	52.2	21.5	26.3
MDA-N		266 GGA-GAA	G to A	266 G/E	m	23	52.7	34.2	13.1
MDA-MB-231/ATCC		280 AGA-AAA	G to A	280 R/K	m	39	54.2	17.5	28.3
MDA-MB-435		266 GGA-GAA	G to A	266 G/E	m	28	48.2	37.8	14
HS 578T		157 GAC-GAA	C to A	157 D/E	m	57			
T-47D		194 CTT-TTT	C to T	194 L/F	m	53			
BT-549						58			
A549/ATCC	Lung	wt		wt	wt	24	39.1	47.4	13.5
NCI-H460		wt		wt	wt	18	51.2	32	16.7
NCI-H23		246 ATG-ATC	G to C	246 M/I	m	37	39.1	33.9	26.9
NCI-H322M		248 CGG-CTG	G to T	248 R/L	m	37	47.1	26.2	26.7
EKVX		del 187–224		del 187–224	m	37	24	25.2	50.8
NCI-H226		309 CCC-GCC	C to G	309 P/A	m	64			
NCI-H522		191 del G		191 del G	m	>50			
HOP-62		ins 212–225		ins 212–225	m	46			
HOP-92		175 CGC-CTC	G to T	175 R/L	m	88			
HCT-116	Colon	wt		wt		18	40.7	31	28.3
HCT-15		wt/153 CCC-GCC	C to G	wt/153P/A	wt/m	21	39.8	34.1	26.1
HT29		273 CGT-CAT	G to A	273 R/H	m	20	33.9	38.9	27.2
HCC-2998		213 CGA-TGA	C to T	213 R/STOP	m	33	45	40.3	14.7
SW-620		273 CGT-CAT	G to A	273 R/H	m	21	44	37.5	18.5
COLO 205		266 GGA-GAA	G to A	266 G/E	m	23	50.9	30.7	18.5
KM12		179 CAT-CGT	A to G	179 H/R	m	23	45.1	24.2	30.7
ACHN	Kidney	wt		wt	wt	31	60.6	17.1	22.4
UO-31		wt		wt	wt	37	46.6	21.8	31.6
RXF-393		175 CGC-CAC	G to A	175 R/H	m	40	46.6	13.4	40
CAKI-1		wt		wt	wt	38	54.3	19.8	25.9
SN12C		336 GAG-TAG	G to T	336 E/STOP	m	30	58.2	20.1	21.6
786-0		278 CCT-GCT	C to G	278 P/A	m	23	39.9	41.2	19
TK-10		264 CTA-CGA	T to G	264 L/R	m	34	35.1	44.9	19.9
A498		wt		wt	wt	65			
OVCAR-4	Ovary	wt		wt	wt	40	41	29.1	29.9
IGROV1		wt		wt		35	62.7	5.1	32.2
OVCAR-3		248 CGG-CAG	G to A	248 R/Q	m	37	41.3	28.3	30.4
OVCAR-8		del 126–132		del 126–132	m	25	50.3	29.2	20.5
OVCAR-5		ins 224		ins 224	m	55	53.3	23	23.7
SK-OV-3		179 CAT-CGT	A to G	179 H/R		57	51	29.1	19.9
SF-539	Central nervous system	wt		wt	wt	34	46.9	42.1	11
SF-295		248 CGG-CAG	G to A	248 R/Q	m	30	73.9	16.9	9.2
SF-268		273 CGT-CAT	G to A	273 R/H	m	34	46.4	32.3	21.2
SNB-75		258 GAA-AAA	G to A	258 E/K	m	40	59.9	16.9	23.2
SNB-19		273 CGT-CAT	G to A	273 R/H	m	35	62	21.3	16.7
U251		273 CGT-CAT	G to A	273 R/H	m	25	41.3	14	44.7
MOLT-4	Leukemia	wt		wt	wt	27	56.6	32.7	10.8
SR		wt		wt		27	51	38.3	10.7
RPMI-8226		285 GAG-AAG	G to A	285 E/L	wt	31	52.8	28.2	19.1
HL-60(TB)		248 CGG-CTG	G to T	248 R/L	m	27	42.3	43.1	14.6
K-562					m	19	41.9	30.7	27.4
CCRF-CEM		248 CGG-CAG	G to A	248 R/Q	m	27	37	48.4	14.5
MALME-3M	Melanoma	wt		wt	wt	35	55.3	29.5	15.2
SK-MEL-5		wt		wt	wt	26	43.8	36.7	19.5
UACC-62		wt		wt	wt	31	75.3	10.2	14.5
LOX IMVI		wt		wt	wt	21	38.4	34.7	26.9
SK-MEL-28		145 TGT-GTT	T to G/G to T	145 C/V	m	36	73.6	11.4	15
M14		266 GGA-GAA	G to A	266 G/E	m	27	40.6	48.3	11.1
UACC-257		wt		wt	wt	>50			
SK-MEL-2		245 GGC-AGC	G to A	245 G/S	wt	>50			
DU-145	Prostate	223 CCT-CTT	C to T	223 P/L		37	52.8	29.3	17.9
PC-3		del 138		del 138	m	29	39.5	37.3	23.2

[a] Determined through complete bidirectional p53 cDNA sequencing using three overlapping PCR primer sets as described in "Materials and Methods."
[b] Transcriptional activity of the DNA binding domain of the p53 cDNA in a yeast-based survival assay determined as described in "Materials and Methods."
[c] Doubling time was calculated from the rate of growth of cells in the sulforhodamine B microtiter plate assay (see "Materials and Methods").
[d] Cell cycle distribution of exponentially growing cultures defined by flow cytometry as described in "Materials and Methods."
[e] wt, wild-type; m, mutant; del, deletion; ins, insertion.

the level of p53 expression in WMN cells (wild-type *p53*): class 1, high basal p53 levels (>2-fold that seen in WMN cells); and class 2, low/negligible basal p53 levels [<2-fold that seen in WMN cells (Table 3)].

Twenty-nine lines (53%) exhibited high basal level expression of p53; of these, 24 lines (89%) contained only mutant *p53*, 3 lines were wild-type for *p53* (OVCAR4, IGROV, SF539), and 1 line (HCT15) was heterozygous for *p53* mutation (Fig. 2 and Table 3).

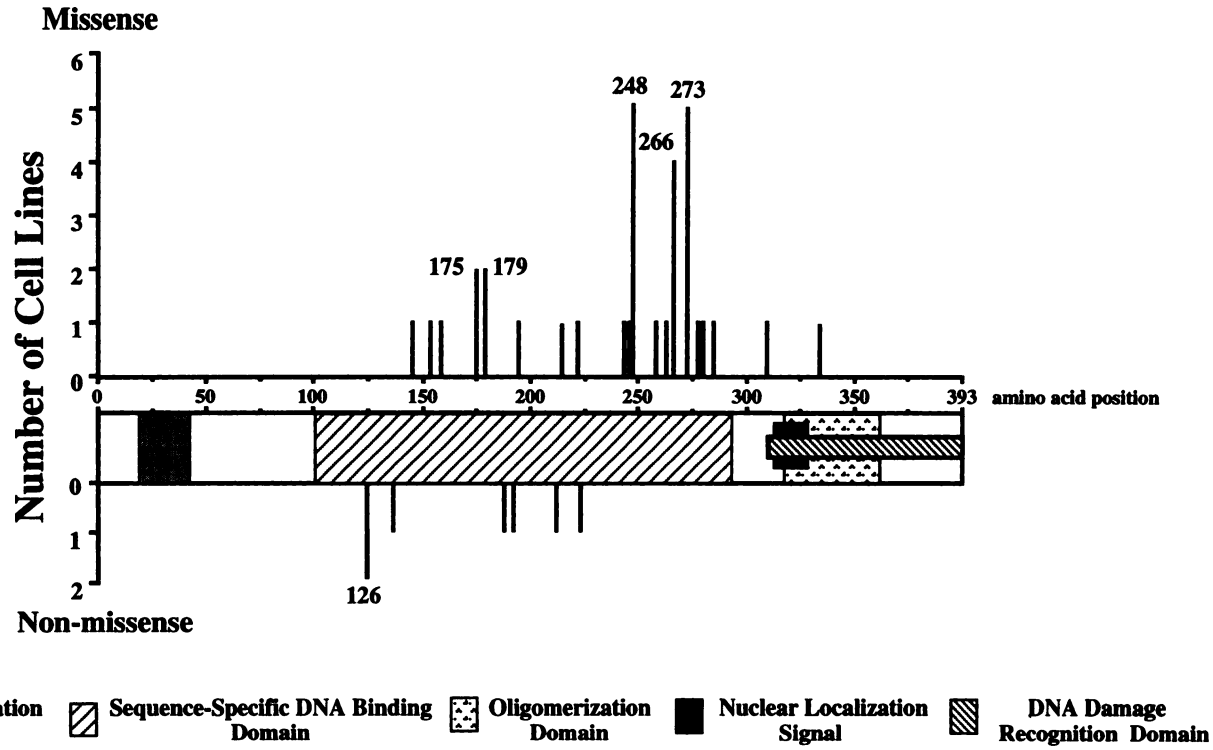

Fig. 1. Spectrum and position of *p53* mutations in cell lines of the NCI anticancer drug screen. Shown is a diagram of the 393 amino acid nuclear *p53* phosphoprotein with functional domains highlighted. The amino-terminal transactivating domain (amino acids 20–42), the central conserved DNA binding domain (amino acids 100–293), and the carboxyl-terminal oligomerization domain (amino acids 319–360) are highlighted, along with nuclear localization sequences (amino acids 316–325) and a putative DNA damage recognition domain (amino acids 311–393). The location of *p53* mutations are shown relative to these functionally important *p53* domains. *Numbers* above and below the *p53* diagram represent numbers of missense and nonmissense (deletion, truncation, or frameshift) mutations, respectively. With the exception of two cell lines (NCI-H226 and SN12C), *p53* mutations were found clustered into the central conserved DNA binding domain of *p53*. *p53* domain structure was redrawn with modifications from Greenblatt *et al.* (33).

Overall, 24 of the 34 mutant *p53* lines tested (71%) overexpressed the mutant p53 protein. Twenty-six lines (47%) exhibited low or negligible basal levels of p53; of these, 10 lines (38%) contained only mutant *p53*, whereas 15 lines (58%) were wild-type for *p53*. Overall 15 of the 18 wild-type *p53* lines tested by Western blotting (83%) expressed barely detectable levels of p53. Eleven of the 13 lines harboring the most frequently observed *p53* codon mutations (codons 248, 266, and 273) showed appreciable p53 accumulation (Fig. 2). Interestingly, KM12 and SKOV3 cells contained the same mutation (179 H/R); however, only KM12 cells exhibited appreciable p53 accumulation. These results coupled with the high level expression of wild-type *p53* in OVCAR4 and SF539 cells suggested that factors other than *p53* sequence might influence the level of p53 within cells.

Assessment of G_1 Arrest following γ-Irradiation and Relationship to *p53* Status. The ability of cells to arrest in G_1 following exposure to 6.3 or 12.6 Gy was assayed in 48 of the 60 cell lines in the NCI screen. Exponentially growing cells were irradiated and then incubated in the presence of the mitotic inhibitor nocodazole to prevent cells that break through the G_2 checkpoint from reentering G_1 (20, 21). G_1 arrest was quantitated as the percentage of the original G_1 population that remained in G_1 for 17 h after irradiation plus incubation with nocodazole. Included in this calculation was subtraction of cells that remained in G_1 in the presence of nocodazole alone. This procedure has previously proven successful in assaying the functional status of the *p53* pathway in a panel of Burkitt's lymphoma and lymphoblastoid cells (20). Fig. 3 illustrates the results of our analyses. As a means of classification, the cell lines were divided into three classes based on the magnitude of G_1 arrest observed following irradiation. For class 1 cells, more than 20% of the original G_1 population had to remain in G_1; we interpreted this response as an indication of a functionally responsive *p53* pathway (20, 36). For class 3 cells, less than 10% of the original G_1 population had to remain in G_1; we interpreted this response as indicating that the *p53* pathway was disrupted in these cells. Class 2 cells showed intermediate G_1 arrest capacity (between 10 and 20% of the original G_1 population).

Table 2 *Type and frequency of p53 mutations in the NCI cell screen lines*

Alteration	No.	%
G to A	17	42
G to T	5	12
C to T	3	7
C to G	3	7
A to G	2	5
T to G	2	5
C to A	1	2.5
G to C	1	2.5
Deletions	5	12
Insertions	2	5
Total	41	100

Of the 48 lines exposed to 6.3 Gy of γ-rays, 9 lines (19%) arrested strongly in G_1, and all of these lines contained wild-type *p53* genes (Fig. 3*B*; Table 1). Thirty-two cell lines (67%) showed minimal or no G_1 arrest at 6.3 Gy, and 29 of these lines (91%) contained mutant *p53* (Fig. 3*B*; Table 1). Seven cell lines (15%) showed intermediate G_1 arrest capacity at 6.3 Gy. Four of these lines contained only wild-type *p53*, and one line (HCT15) contained a heterozygous *p53* status. By increasing the radiation dose by a factor of 2 (to 12.6 Gy), we found that the degree of G_1 arrest in cells with wild-type *p53* generally increased above that seen at 6.3 Gy (Fig. 3). Of the 38 lines exposed to 12.6 Gy of γ-rays, 14 (37%) arrested strongly in G_1, and all of these

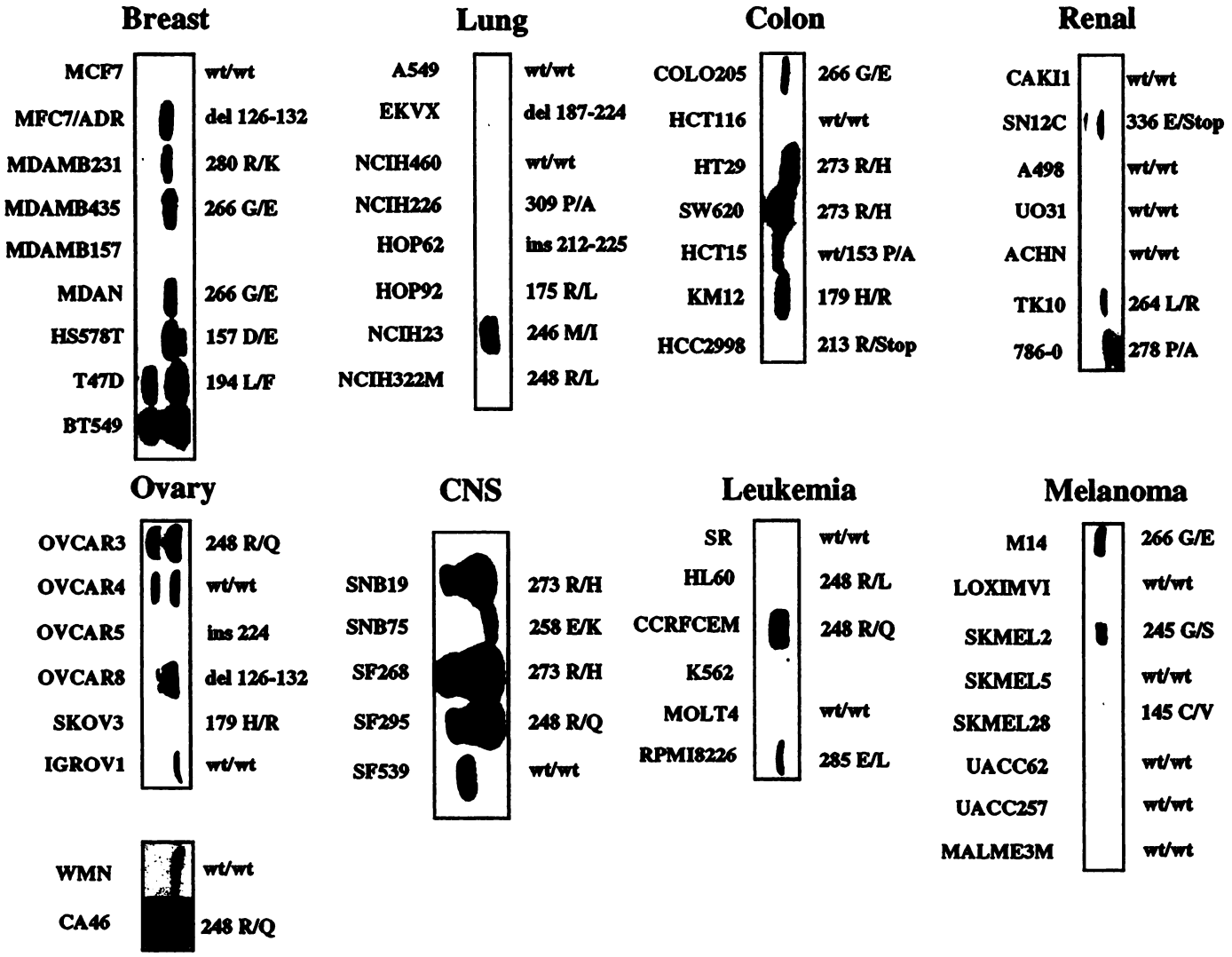

Fig. 2. Western blotting of basal p53 protein levels in 55 of the NCI cell screen lines. Cell lysates prepared from exponentially growing cells were subjected to SDS-PAGE and then Western blotted using the p53 monoclonal antibody Pab1801. Comparison between individual blots was accomplished by including 100 μg of total cell protein from the wild-type *p53* cell line WMN and the mutant *p53* cell line CA46 (248 R/Q) on each blot (Refs. 20 and 21; sample *inset* at base of figure). Protein from one additional breast cell line, MDAMB157, not in the NCI panel, was also included in the Western blot on the breast cancer cell lines.

14 lines contained wild-type *p53*. Twenty-two of the cell lines (58%) showed minimal G_1 arrest at 12.6 Gy, and all but 2 (9%) contained mutant *p53*. Only 2 lines (5%) showed intermediate G_1 arrest at 12.6 Gy, and both of these contained mutant *p53*.

The yeast growth assay suggested that RPMI8226 cells contained transcriptionally active *p53* despite a mutation at codon 285 (E/L). These cells, however, failed to arrest in G_1 following γ-irradiation (Fig. 3), suggesting that the *p53* pathway was defective in this line. The CNS cell line SN12C, which harbored a *p53* mutation outside of the sequence specific DNA binding domain of *p53* (codon 336: E to stop), also failed to arrest in G_1. This result was consistent with the lack of activity of *p53* cDNA from SN12C cells in the yeast survival assay (Table 1).

Table 3 *Basal level expression of p53 protein in the NCI cell screen lines*

	Basal level of p53 protein[a]		
p53 sequence	High	Low	Total
wt/wt[b]	3	15	18
mutant	24	10	34
wt/mutant	1		1
ND	1	1	2
Total	29	26	55

[a] The basal levels of p53 in each line were classified into two groups according to the level of p53 expression in WMN cells (wild-type p53). Lower negligible basal p53 level, <2-fold that seen in WMN cells; high basal p53 level, ≥2-fold that seen in WMN cells.
[b] wt, wild type; ND, not determined.

Effect of γ-Irradiation on *CIP1/WAF1*, *GADD45*, and *MDM2* mRNA Levels and Relationship to *p53* Status. The functional status of the *p53* pathway in the 60 cell lines of the NCI screen was also assessed by measuring the γ-ray inducibility of three *p53*-regulated genes, *CIP1/WAF1*, *GADD45*, and *MDM2*. Exponentially growing cells were irradiated with 20 Gy of γ-rays, and 4 h later, polyadenylated mRNA was extracted from each line and subjected to a quantitative dot-blot hybridization assay (30, 31). The degree of induction of each transcript was related to basal expression levels, and equivalent mRNA loadings were ensured by also assaying for the constitutively expressed housekeeping gene, glyceraldehyde-3-phosphate dehydrogenase (see "Materials and Methods"). The cell lines were categorized into three groups based on the magnitude of mRNA induction for each transcript. Class 1 cells were those that exhibited strong mRNA induction (>4-fold above basal levels), and such a response was interpreted as indicative of a functionally responsive *p53* pathway in such cells. Class 3 cells were those that showed minimal or no mRNA

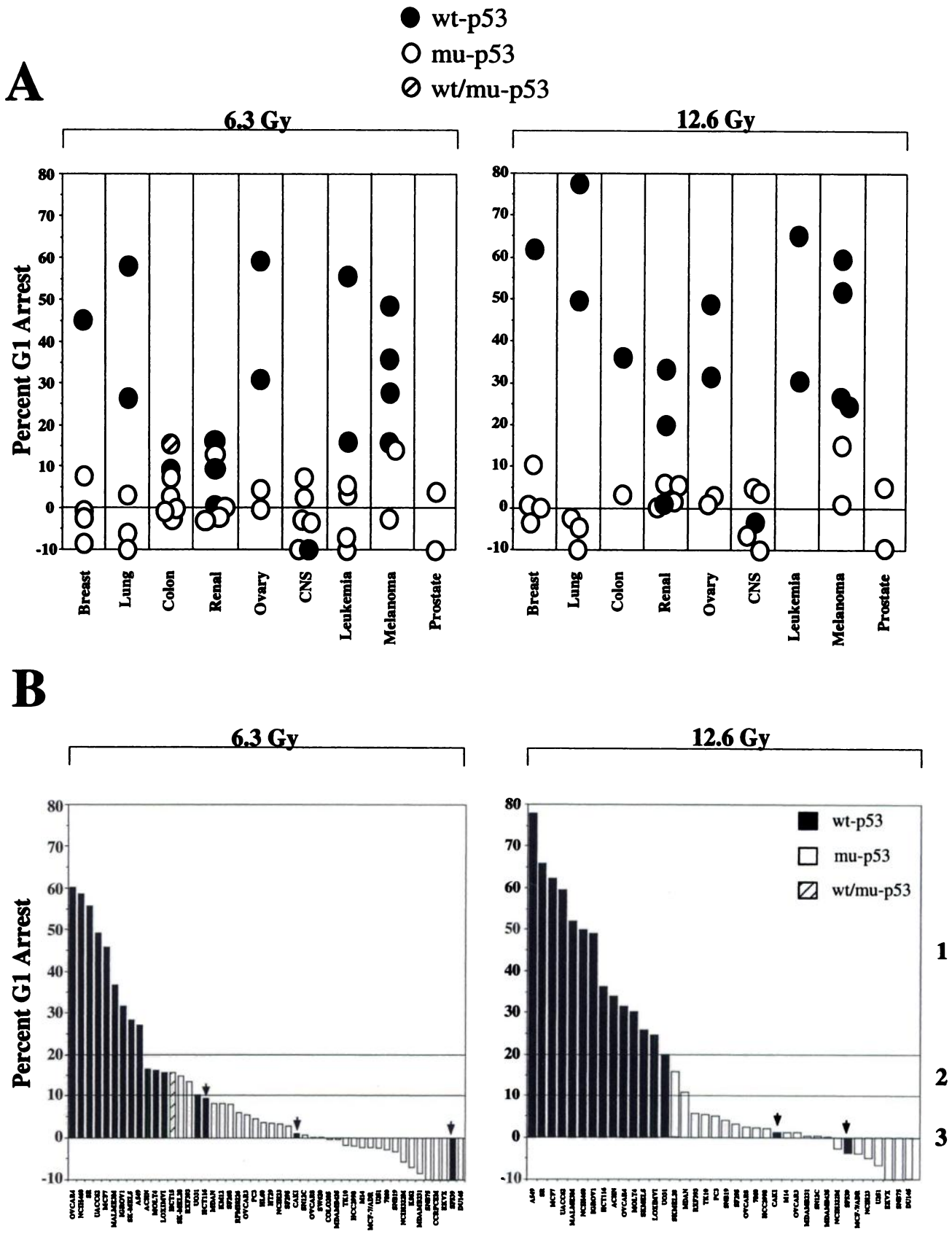

Fig. 3. Degree of G_1 arrest induced by 6.3 or 12.6 Gy of γ-rays in 48 of the NCI cell screen lines. *A*, percentage of the original G_1 population that remained in G_1 for 17 h following exposure to 6.3 or 12.6 Gy of γ-irradiation. Cell cycle distribution was quantitated using flow cytometry as described in "Materials and Methods." Measurements shown were made in the presence of the mitotic inhibitor nocodazole to ensure that cells that broke through the G_2 checkpoint did not reenter G_1. The individual cell lines have been grouped according to the tissue of origin for each line. *B*, ranked order of G_1 arrest induced by 6.3 or 12.6 Gy of γ-irradiation. G_1 arrest responses were grouped into three classes: class 1 cells showed strong G_1 arrest (>20% of the original G_1 population); class 2 cells showed intermediate G_1 arrest (10–20% of the original G_1 population); and class 3 cells showed weak or no G_1 arrest (<10% of original G_1 population). Twelve lines were deemed to grow too slowly for the G_1 arrest test and were not included in the analysis (Table 1). *Arrows*, wild-type *p53* lines showing weak or no G_1 arrest.

induction (<2-fold above basal levels), and such a response was interpreted as a sign of *p53* dysfunction. Class 2 cells showed intermediate mRNA induction levels (between 2-fold and 4-fold).

Of the 60 cell lines assayed for γ-ray inducibility of *CIP1/WAF1* mRNA, 18 lines (30%) showed strong induction of this transcript (class 1), and with the exception of SNB19 cells (258 E/K) all of these lines contained wild-type *p53* sequence (Fig. 4). The only wild-type *p53* line that did not exhibit *CIP1/WAF1* mRNA induction was A498. The slowly growing nature of this line (doubling time, 67 h) prevented accurate measurement of G_1 arrest by flow cytometry. Thirty-nine cell lines (65%) failed to induce *CIP1/WAF1* mRNA following exposure to 20 Gy of γ-rays (class 3), and 36 of these lines (92%) contained mutant *p53* (Fig. 4). The two remaining lines that lacked CIP1/*WAF1* mRNA induction were HCT15 cells, which contained a heterozygous *p53* mutation, and BT549 cells, which have previously been reported to harbor mutant *p53* (18).

Strong γ-ray induction of *GADD45* mRNA (class 1) was observed in six cell lines (10%), all of which contained wild-type *p53* (Fig. 5). Eight lines induced *GADD45* mRNA to levels between 2-fold and 4-fold, and *p53* sequencing data on six of these lines revealed wild-type *p53* sequence (Table 1). Taken together, 11 of the 18 wild-type *p53* cell lines (61%) assayed demonstrated moderate to strong (>2-fold) induction of *GADD45* mRNA. The degree of *GADD45* mRNA induction was therefore less precise in pinpointing wild-type *p53* cell lines compared to similar assessments on the level of *CIP1/WAF1* mRNA induction. This appeared to be due to four melanoma (UAC257, SKMEL5, UACC62, and LOX) and two renal cell lines (CAKI and A498), all of which contained wild-type *p53* but showed limited or no induction of *GADD45* mRNA following γ-irradiation. Lack of *GADD45* mRNA induction occurred despite the strong induction of *CIP1/WAF1* mRNA in five of these cell lines (compare Figs. 4 and 5; see Ref. 37). G_1 arrest assays performed on three of these lines (UACC62, SKMEL5, and LOX) also showed moderate to strong induction of G_1 arrest (Fig. 4). Our results indicated that a possible defect(s) in these lines resides at the level of *GADD45* induction (37). Forty-six cell lines failed to show induction of *GADD45* mRNA (class 3) following γ-irradiation; of these, 39 cell lines (85%) contained mutant *p53*, 6 lines (13%) contained wild-type *p53*, and one cell line, HCT15, was heterozygous for *p53* mutation.

With the exception of one cell line (ACHN), the degree of *MDM2* mRNA induction observed in cells with wild-type *p53* was generally weaker than that observed for either *CIP1/WAF1* or *GADD45* (compare the *Y*-axis values of Figs. 4, 5, and 6). Of the 12 cell lines that induced *MDM2* mRNA above 2-fold, 9 (75%) were wild-type for *p53*, and 3 lines (25%) were mutant for *p53* (Fig. 6). The mutant *p53* lines that exhibited moderate induction of *MDM2* mRNA were SF295, CCRFCEM, and HL60 cells. Although the remaining nine wild-type *p53* lines assayed showed relatively weak or no MDM2 induction (<2-fold), the majority of these lines (six of nine) showed *MDM2* mRNA induction of between 1.5-fold and 2-fold. A comparable level of *MDM2* mRNA induction was seen in only 1 of the remaining 37 mutant *p53* lines tested. These results illustrate that when the level of *MDM2* mRNA induction was set at 1.5-fold or above, transcriptional activation of *MDM2* can pinpoint 83% of the wild-type *p53* cell lines tested.

Correlations between the *p53* cDNA Status of the 60 Cancer Cell Lines of the NCI Screen and the Growth-Inhibitory Potency of Bleomycin, 5-Fluorouracil, and Cisplatin. We first investigated whether *p53* cDNA status could explain differences in the sensitivity of the 60 cancer lines in the NCI screen to bleomycin, 5-fluorouracil, and cisplatin. Fig. 7 shows the dose of each of these agents required to inhibit growth of the cells by 50% with respect to the vehicle-treated control population (GI_{50}). Data on the sensitivity of the cell lines to each agent are plotted according to the status of *p53* cDNA sequence (Table 1). Eighteen wild-type *p53* and 39 mutant *p53* cell lines were assessed in each case, and each point on the graphs in Fig. 7 represents the averaged GI_{50} from multiple experiments for an individual cell line treated with that agent. The *solid bars* (Fig. 7) shown within each plot represent the median response of each group of cell lines. We found that when taken together as a group, the mutant *p53* cell lines tended to be less sensitive to bleomycin-, 5-fluorouracil-, and cisplatin-induced growth inhibition than the wild-type *p53* cell lines. The median GI_{50} for the group of mutant *p53* lines treated with bleomycin was approximately 2.5 μM, compared to approximately 0.25 μM for the group of wild-type *p53* cell lines (10-fold difference). The median GI_{50} for the group of mutant *p53* lines treated with 5-fluorouracil was approximately 25 μM, compared to approximately 4 μM for the group of wild-type *p53* cell lines (6-fold difference), and the median GI_{50} for the group of mutant *p53* lines treated with cisplatin was approximately 5 μM, compared to 1.5 μM for the group of wild-type *p53* cell line (3.3-fold difference).

Included in Fig. 7 are values obtained from the Wilcoxon rank sum test (p value = 0.996–0.999). If the p values derived from this nonparametric test were to be interpreted statistically, then values >0.975 or <0.025 would be required to reject the null hypothesis of equal potencies for the *p53* mutant and wild-type lines for any given agent. Because the 60 cell lines do not, however, represent a random sample from a definable underlying population, the p values should be considered simply as a convenient parameter for describing tendencies in the data. For example, a p value of 0 indicates a compound that tended to be more potent in the *p53* mutant lines; a p value of 1 indicates a compound that tended to be more potent in the *p53* wild-type lines; a p value of 0.5 indicates no trend in either direction. The Wilcoxon rank-sum test supported the observed tendency of the mutant *p53* lines to be less sensitive to bleomycin, 5-fluorouracil, and cisplatin compared to the wild-type *p53* cell lines (bleomycin, p value = 0.999; 5-fluorouracil, p value = 0.996; cisplatin, p value = 0.998).

In the case of bleomycin or 5-fluorouracil, only 2 of the 18 wild-type *p53* lines exhibited less sensitivity to these agents than the median for the mutant *p53* cell lines, and only 5 of 39 mutant *p53* lines (13%) exhibited greater sensitivity to these agents than the median value for the wild-type *p53* cell lines (Fig. 7). In the case of cisplatin, only 1 of the 18 wild-type *p53* lines exhibited less sensitivity to cisplatin than the median for the mutant *p53* cell lines, and only 7 of 39 mutant *p53* lines (18%) exhibited greater sensitivity to cisplatin than the median for the wild-type *p53* cell lines (Fig. 7). Taken together, these findings support an observed trend in the data that suggested that when taken as a group, the mutant *p53* cell lines tended, in this assay, to be less sensitive to bleomycin-, 5-fluorouracil-, and cisplatin-induced growth inhibition than the wild-type *p53* cell lines.

Despite this trend in the data, there was a fair degree of spread in the range of GI_{50}s for either the group of wild-type *p53* lines or the mutant *p53* lines. This spread could not be accounted for on the basis of differences in the doubling time for each cell line or upon the cell cycle distribution patterns of exponentially growing cells at the start of treatment (Table 1 and data not shown). We investigated whether any additional *p53* parameters might help explain the spread of responses within each group to the drug cisplatin. In the case of the mutant *p53* lines, we could not significantly account for this spread on the basis of subdividing the mutant *p53* lines according to (*a*) p53 protein expression levels, (*b*) missense *versus* nonmissense mutations, or (*c*) hot spot *versus* non-hot spot mutations (data not shown). Subdivision on the basis of the position of the amino acid mutation was not possible due to the small sample size for each mutation (Fig.

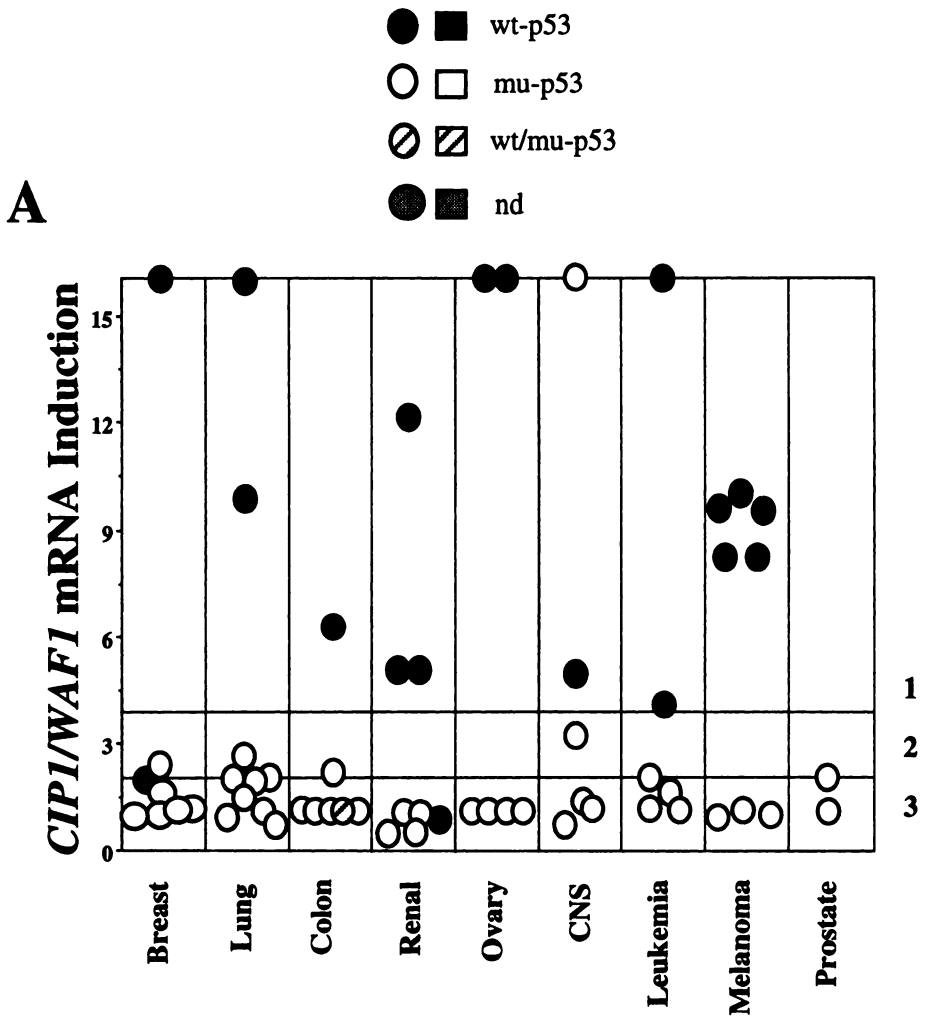

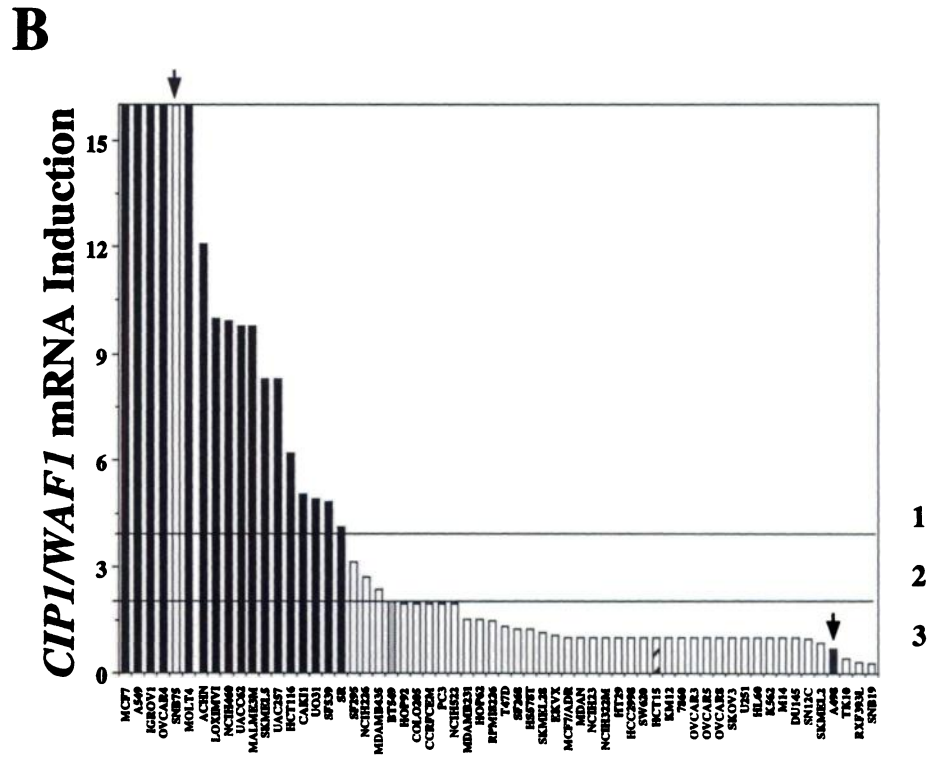

Fig. 4. Degree of γ-ray inducibility of *CIP1/WAF1* mRNA in 60 lines from the NCI screen. *A*, exponentially growing cells were exposed to 20 Gy of γ-rays; 4 h later, cells were lysed, and polyadenylated mRNA was extracted from a control or an irradiated sample for each line. *CIP1/WAF1* mRNA levels were assayed using a quantitative dot-blot procedure (see "Materials and Methods"). Shown is the degree of *CIP1/WAF1* mRNA induction relative to basal levels of this transcript ordered according to tissue type. *B*, ranked order of *CIP1/WAF1* mRNA induction. The degree of *CIP1/WAF1* mRNA induction was grouped into three classes: class 1 cells showed strong induction of *CIP1/WAF1* mRNA (>4-fold above basal levels); class 2 cells showed intermediate induction of *CIP1/WAF1* mRNA (between 2-fold and 4-fold); and class 3 cells showed weak or no induction of *CIP1/WAF1* mRNA (<2-fold). The *Y* axis has been limited to 16-fold mRNA induction above basal levels. *Arrows*, cell lines showing unusual *CIP1/WAF1* mRNA induction responses.

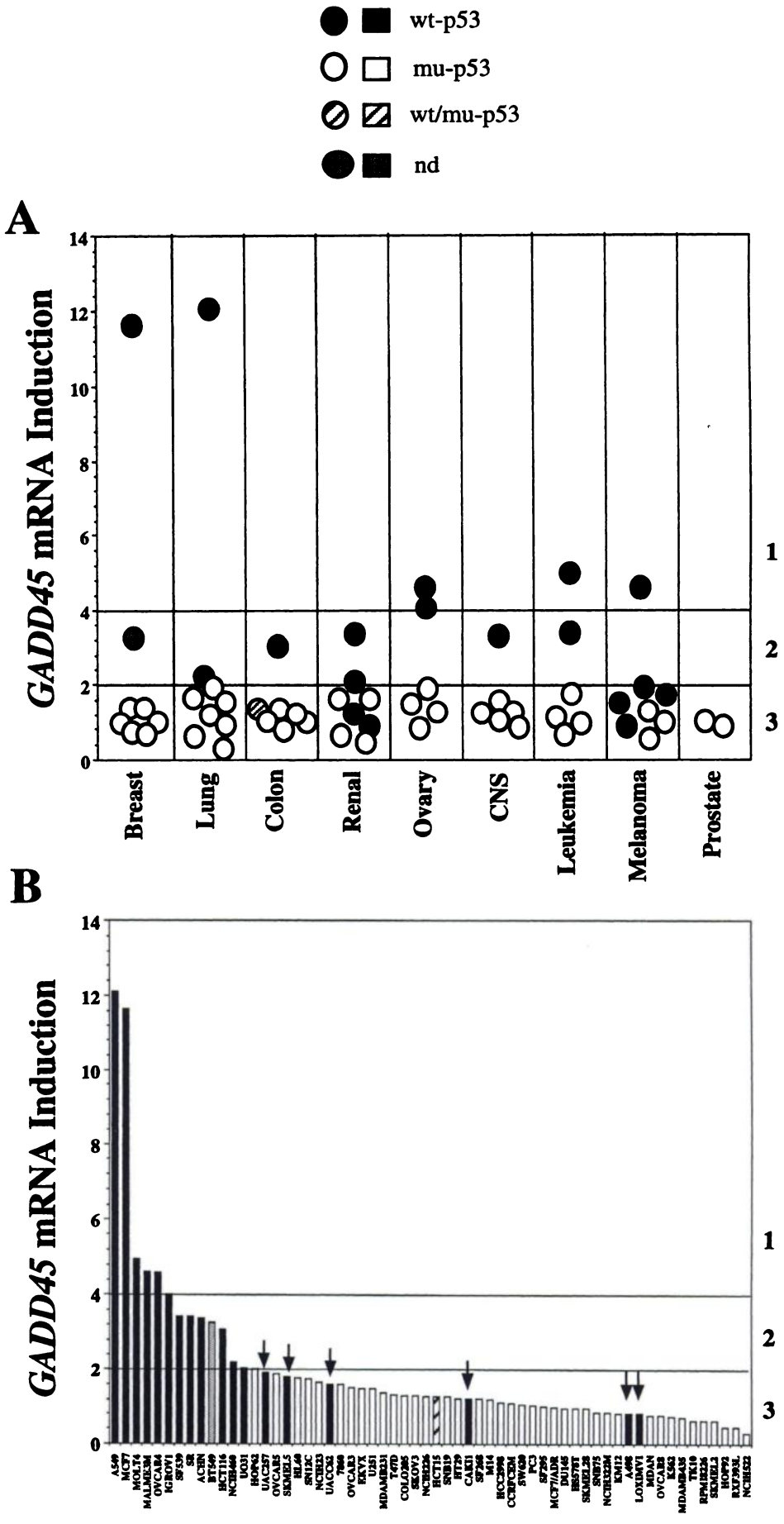

Fig. 5. Degree of γ-ray inducibility of *GADD45* mRNA in 60 lines from the NCI screen. *A*, degree of *GADD45* mRNA induction relative to basal levels of this transcript ordered according to tissue type. GADD45 mRNA levels were assayed as described in the legend of Fig. 4 and "Materials and Methods." *B*, ranked order of *GADD45 mRNA* induction. The degree of *GADD45* mRNA induction was grouped into three classes as described in the legend of Fig. 4 and "Materials and Methods." *Arrows*, cell lines showing reduced or negligible *GADD45* mRNA induction responses despite containing wild-type *p53*.

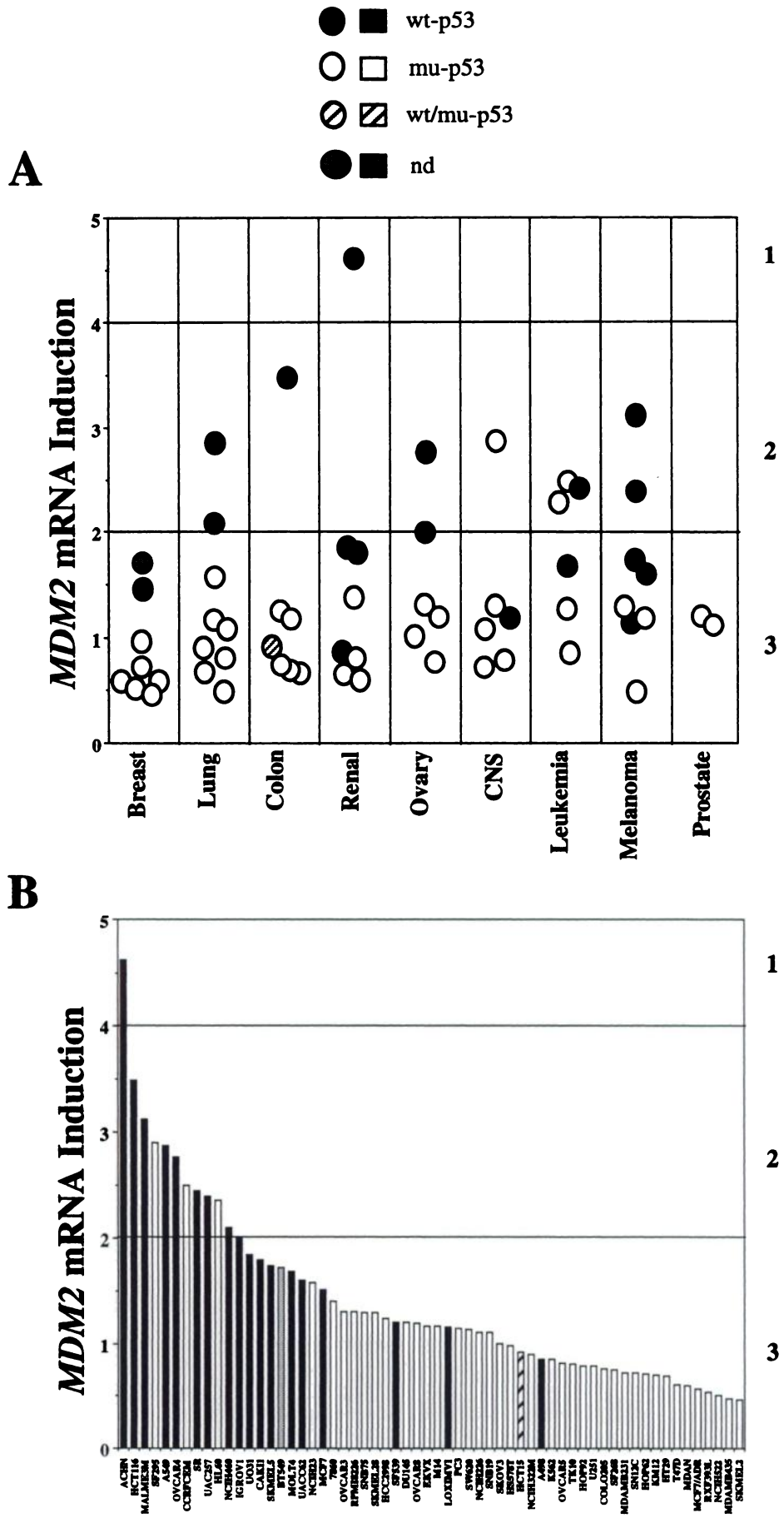

Fig. 6. Degree of γ-ray inducibility of *MDM2 mRNA* in 60 lines from the NCI screen. *A*, degree of *MDM2* mRNA induction relative to basal levels of this transcript, ordered according to tissue type. MDM2 mRNA levels were assayed as described in the legend of Fig. 4 and "Materials and Methods." *B*, ranked order of *MDM2 mRNA* induction. The degree of *MDM2* mRNA induction was grouped into three classes as described in the legend of Fig. 4 and "Materials and Methods."

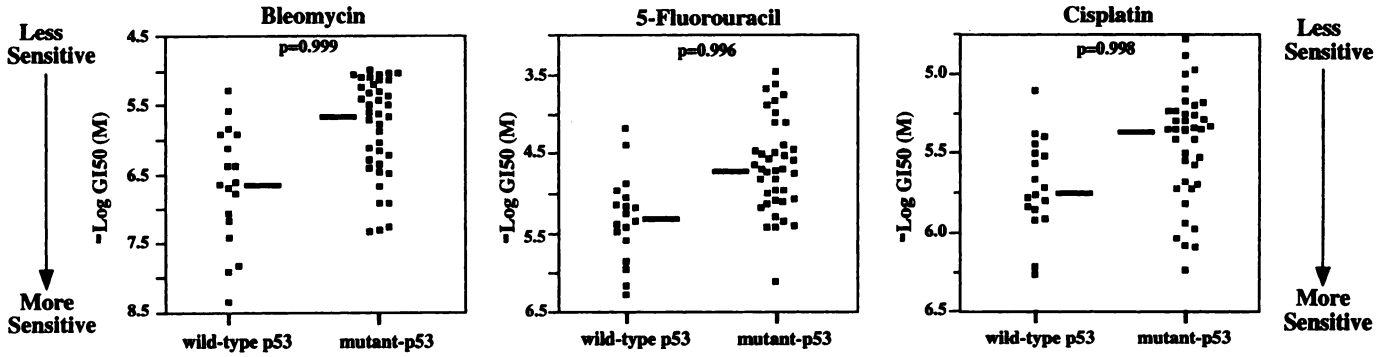

Fig. 7. Relationship between *p53* gene sequence and chemosensitivity of the NCI cell screen lines to bleomycin, 5-fluorouracil, and cisplatin. Shown are the sensitivities of the individual cell lines in the NCI screen plotted according to *p53* cDNA sequence (Table 1). Sensitivity is plotted as GI_{50}. A negative log (GI_{50}) value of 6 corresponds to a concentration of 10^{-6} M. The *solid bar* shown next to each group of data points represents the median log (GI_{50}) value for that group of cell lines. The *P* shown for each drug was generated from a one-tailed Wilcoxon rank-sum test and indicates the significance of the difference in median responses between the wild-type and the mutant *p53* cell lines.

1). In the case of the wild-type *p53* lines, we again could not significantly account for the spread in responses to cisplatin on the basis of subdividing the wild-type *p53* lines according to (*a*) the strength of G_1 arrest or (*b*) induction of the *p53*-regulated genes *CIP1/WAF1*, *GADD45*, and *MDM2* (data not shown). These findings suggested that factors in addition to the ones we measured contributed to the final variation in the GI_{50}s. This was not unexpected, based on the multigenetic nature of human cancer and the presumed variable genetic background of these individual cancer cell lines. A full multivariate analysis using additional molecular characteristics being assessed for the lines might help to explain this spread of responses for cisplatin and the larger set of compounds tested in the NCI screen.

Correlations between the Complete Set of *p53* Status Measurements Recorded on the NCI Screen Cell Lines and the Growth-Inhibitory Potency of 123 Standard Agents. The complete set of *p53* assessments gathered on the NCI screen lines were next used to probe a database of growth-inhibitory potencies for 123 standard agents, which included the majority of clinically approved anticancer drugs. These agents make up a standard set of compounds that have been tested against the lines on multiple occasions and for which the mechanism of action of each had previously been assigned (5, 8, 10). As a matter of convenience in illustrating the correlations uncovered, we color coded the *P*s generated by the Wilcoxon rank sum test according to a scale illustrated in Fig. 8. This scale provides a simple means of rapidly assessing patterns in the complex data according to a color coding. For example, red indicates an agent that tended to inhibit growth of the *p53* wild-type lines to a greater extent than the group of mutant-*p53* cell lines in this assay. Violet indicates an agent with the opposite tendency. Each *vertical column* in Fig. 8 represents the activity of an individual agent, and each *horizontal row* indicates a particular *p53* status measurement. The 123 agents shown in Fig. 8 were grouped into five classes based on putative mechanism of action: alkylating agents, DNA antimetabolites, RNA antimetabolites, topoisomerase I and II inhibitors, and antimitotic agents. These assignments were made previously without prior knowledge of cell screen results (5, 8).

In the case of *p53* cDNA sequence, a large proportion of agents in the first four mechanism classes exhibited a red color code, indicating that they tended to inhibit growth of the wild-type *p53* lines more than that of the mutant *p53* lines (Fig. 8). Agents included in this class were: (*a*) DNA cross-linking agents, such as cisplatin, carboplatin, nitrogen mustard, and thiotepa; (*b*) DNA/RNA antimetabolites, such as 5-fluorouracil and methotrexate; (*c*) topoisomerase I inhibitors, such as camptothecin; and (*d*) topoisomerase II inhibitors, such as adriamycin. Similar correlations were seen when results from the yeast growth assay or γ-ray induction of *CIP1/WAF1* or *MDM2* or the level of γ-ray-induced G_1 arrest at 12.6 Gy were used as factors to search for chemosensitivity relationships (Fig. 8).

Somewhat weaker correlations were seen for *GADD45* mRNA induction and G_1 arrest at 6.3 Gy. This might be due to the fact that these two measurements were less effective at predicting wild-type *p53* cDNA status than were the other *p53* measurements we recorded (*p53* cDNAs in the yeast growth assay, γ-ray induction of *CIP1/WAF1* or *MDM2*, and γ-ray-induced G_1 arrest at 12.6 Gy). Indeed, in the case of *GADD45* mRNA induction, there were six cell lines (UACC257, SKMEL5, UACC62, CAKI1, A498, and LOXIMVI) that exhibited minimal or no *GADD45* mRNA induction following irradiation despite containing wild-type *p53* sequence (Fig. 5). Five of these cell lines had robust induction of *CIP1/WAF1* mRNA, whereas one (A498) was deficient in *CIP1/WAF1* mRNA induction. In the case of G_1 arrest, in which we applied a cutoff of >20% G_1 arrest for intact *p53* function (Fig. 3), only 9 of 16 wild-type *p53* lines tested were accurately predicted to be wild-type *p53*, whereas 14 of the 16 cell lines were accurately predicted to be wild-type *p53* at 12.6 Gy.

Correlations uncovered when p53 protein expression levels were used tended to be opposite those obtained with the wild-type *p53* cDNA sequence (Fig. 8). This was not unexpected, because the majority of the mutant *p53* cell lines analyzed (>70%) overexpressed the mutant p53 protein (Fig. 2).

In contrast to most of the compounds in the four mechanism of action classes described above, we found that the activity of the antimitotic compounds, such as paclitaxel, vincristine, and vinblastine did not correlate with any of the *p53* status measurements we made (Fig. 8). By way of example, the individual cell line responses to paclitaxel, grouped according to *p53* cDNA status, are shown in Fig. 9. The results suggest that for the majority of agents within the antimitotic class, *p53* status was not a major predictor of growth-inhibitory activity in the NCI screening assay.

DISCUSSION

This study reports (*a*) the status of the *p53* tumor suppressor pathway in 60 cancer cell lines used in the NCI anticancer drug screen, and (*b*) relationships between *p53* status and the activity of 123 standard agents, the mechanisms of drug action of which have previously been assigned (5, 8, 10). The *p53* characterization data reported here has also made possible a recent information-intensive approach to the molecular pharmacology of cancer as it relates to the *p53* tumor suppressor pathway in the NCI cell screen cell lines (38).

Complete bidirectional *p53* cDNA sequencing on 58 of the 60 cell

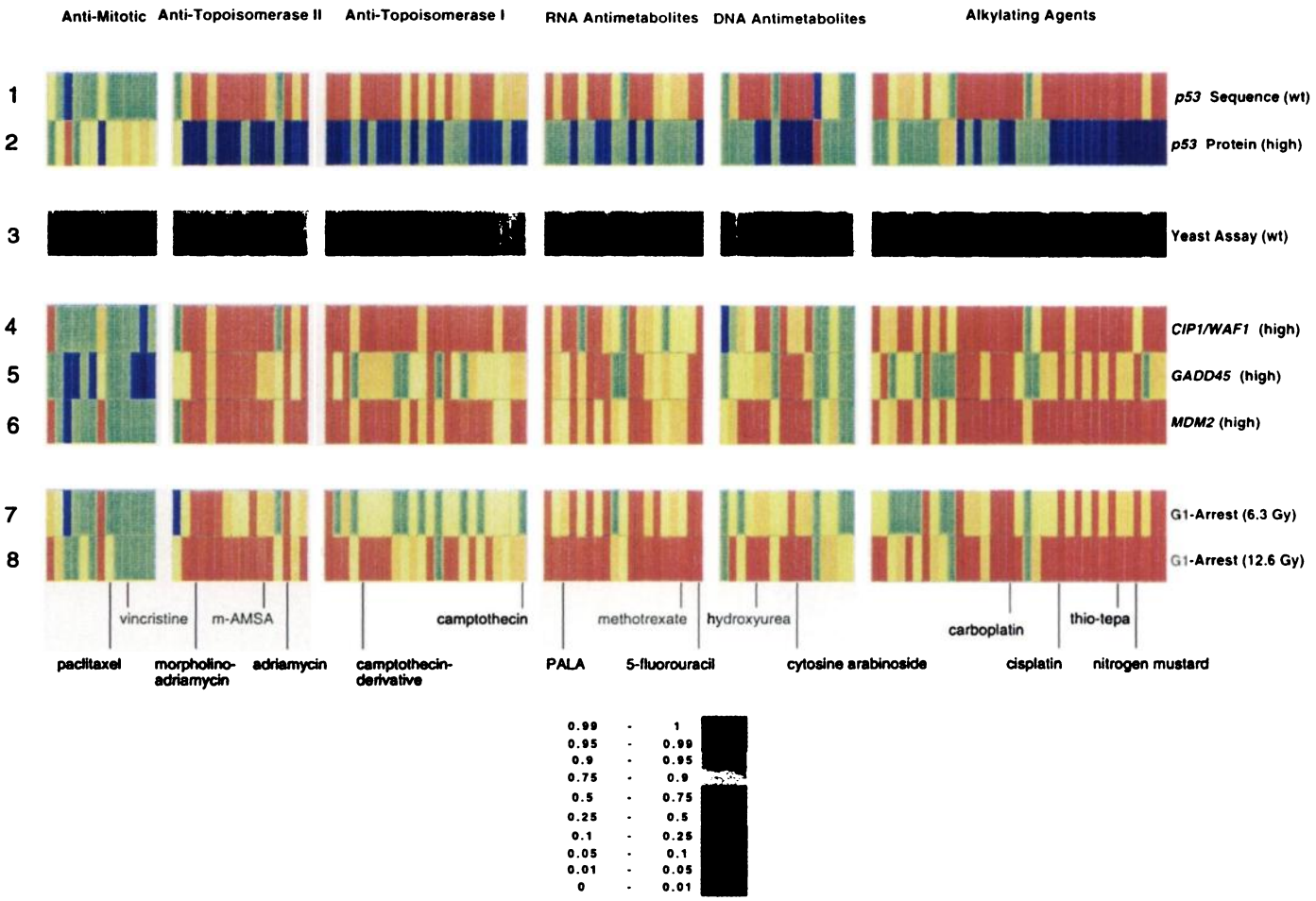

Fig. 8. Wilcoxon *P* matrix relating the activity of 123 agents with assigned mechanism of drug action to *p53* status measurements. *P*s derived from the Wilcoxon rank-sum test indicate the apparent dependence of the activity of a drug on each *p53*-pathway component. The values have been color coded according to the scale shown in the figure. For each drug, *red* indicates higher sensitivity in the group of human cell lines defined as normal *p53* according to the following criteria: *p53* wild-type sequence; wild-type *p53*-like activity in the yeast assay; *CIP1/WAF1* mRNA induction greater than 2-fold; *GADD45* mRNA induction greater than 2-fold; *MDM2* mRNA induction greater than 1.5-fold; G_1 arrest at 6.3 Gy greater than 20%; and G_1 arrest at 12.6 Gy greater than 20%. Cells exhibiting high basal expression of p53 tended to differ in their responses to these compounds compared to cells defined as normal *p53*. These results are consistent with the high frequency with which mutant *p53* sequence was found in cells expressing high basal levels of p53 (see Fig. 2 and Table 3). The proposed mechanism of action of each group of compounds is shown at the *top* of the figure (the term "alkylating agents" is used broadly and includes platinating agents, such as cisplatin). Some sample compounds from each of these groups have been highlighted along the base of row 8. The scale at the *bottom* shows the color-coding of *P*s, ranging from $P = 0$ to $P = 1$.

lines in the NCI anticancer drug screen revealed that 18 lines contained wild-type *p53* sequence, 39 lines contained only mutant *p53*, and 1 line was heterozygous for *p53* mutation (Table 1; Fig. 1). The overall frequency with which mutant *p53* status was observed in the NCI screen cell lines (68%) was similar to that observed in cell lines derived from Burkitt's lymphoma (39), head and neck cancer (40), colon cancer (41) and lung cancer (42). In each case, however, the frequency with which mutant *p53* status was observed in the cancer cell lines was somewhat higher than that found in primary tumor samples (Ref. 33 and references therein). Consistent with the relative infrequency of *p53* mutations in primary melanoma and renal cancer (Ref. 33 and references therein), we found that the melanoma and renal cell line panels in the NCI screen had a relatively higher number of wild-type *p53* lines [9 wild-type *p53* lines of 16 (56%)] compared to the remaining tissue panels [9 wild-type *p53* lines of 41 (22%)].

The majority of *p53* sequence mutations observed in the NCI screen lines were missense mutations, and approximately 73% of these mutations occurred at G:C base pairs (Table 1; Fig. 1). The most frequent base alterations were G/A (41% of cases) and G/T (12%) replacements (Fig. 1), and the frequency with which these changes occurred was similar to that observed in an analysis of 2567 primary tumor samples (G/A, 41%; G/T, 17%; Ref. 33). This was also the case for deletion/insertion mutations (NCI screen lines, 17%; primary tumor samples, 13%; Ref. 33). In agreement with previous studies (Refs. 18 and 33 and references therein), the majority of *p53* mutations were clustered into the central evolutionarily conserved DNA binding domain of *p53*. Within this region, a number of hot spot *p53* mutations were observed, including mutations at amino acids 248 and 273 (which do not significantly affect p53 structure; Ref. 43 and references therein). In the crystal structure of the p53-DNA complex, these amino acids make contacts with the DNA (43). Two cell lines had mutations at arginine-175, and two lines had mutations at histidine-179 (one of the four zinc binding sites in p53). Both of these residues appear to be critical in stabilizing p53 conformation, and mutations at these sites have previously been associated with a denatured p53 structure (Ref. 43 and references therein).

The yeast-based survival assay provided a means of directly assessing the functional significance of each *p53* mutation (28). This assay selects for a transcriptionally competent *p53* sequence (see "Materials and Methods"). Of the 38 mutant *p53* cell lines assayed, 36 (95%) lacked transcriptional activity in the yeast assay. The two mutant *p53* lines deemed wild-type *p53* in the yeast assay (RPMI8226, 285 E/L; SKMEL2, 245 G/S) failed to exhibit γ-ray-induced G_1 arrest and/or γ-ray-induced expression of *CIP1/WAF1* or

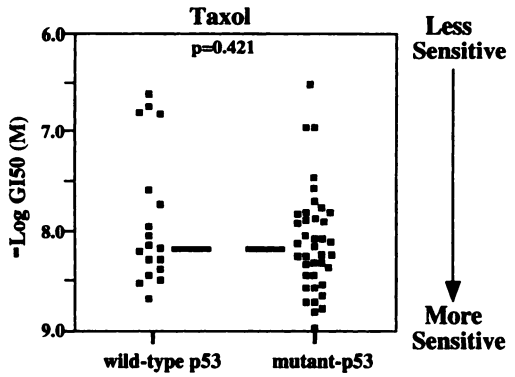

Fig. 9. Relationship between *p53* gene sequence and chemosensitivity of the NCI cell screen lines to paclitaxel. Shown are the sensitivities of the individual cell lines in the NCI screen plotted according to *p53* cDNA sequence (Table 1). Sensitivity is plotted as the dose of paclitaxel required to inhibit growth of the cells by 50% with respect to the vehicle-treated control population (GI_{50}). A negative log (GI_{50}) value of 6 corresponds to a concentration of 10^{-6} M. The *solid bar* shown next to each group of data points represents the median negative log (GI_{50}) value for that group of cell lines. The *P* shown for paclitaxel was generated from a one-tailed Wilcoxon rank-sum test and indicates no significance in the difference in median responses between the wild-type and the mutant *p53* cell lines.

GADD45 mRNA. The discrepancy between the yeast assay and functional tests in RPMI8226 and SKMEL2 cells might be explainable if the mutations were temperature sensitive, because the lower temperature at which the yeast assay is performed might favor a wild-type p53 conformation (28). Alternatively, these particular mutants may have been false positives in the yeast assay used, or these two cell lines could harbor other defects in the *p53* pathway. The yeast assay was successful in determining the heterozygous *p53* nature of HCT-15 cells, as well as all of the wild-type *p53* cell lines assayed. Overall, the success rate of the yeast assay in determining *p53* status was 96%.

Assessment of basal p53 protein levels revealed that 70% of the NCI cell screen lines containing mutant *p53* sequence expressed elevated basal levels of the mutant p53 protein. Interestingly, three wild-type *p53* lines (OVCAR4, IGROV1, and SF539) also expressed appreciable basal levels of p53. p53 protein determinations were thus not always effective in establishing *p53* gene status. Of the NCI screen lines that contained hot spot mutations, all of those with a 248 R/Q (3 lines), 273 R/H (4 lines), or 266 G/E (4 lines) mutation expressed elevated p53 protein levels. Curiously, two cell lines that contained a 248 mutation that changed an arginine to leucine, instead of to glutamine, did not accumulate p53 (Fig. 2). Comparisons between mutations expected to alter p53 conformation (175 R/H and 179 H/R) and those that would not (248 R/Q and 273 R/H) did not reveal a consistent basis for *p53* accumulation in these cancer cell lines. Also, KM12 and SKOV3 cells exhibited different p53 levels despite the fact that both contained a 179 H/R mutation that would destabilize p53 structure (Ref. 43 and references therein). These results suggest that other cellular factors may also govern to the accumulation of mutant p53 protein in cells.

A requirement for wild-type *p53* sequence in γ-ray-induced G_1 arrest in cell lines from the NCI screen supports earlier reports that established the significance of *p53* in regulating the G_1 checkpoint response to DNA damage (36). We found that only 2 of the 16 wild-type *p53* lines tested at 12.6 Gy of γ-rays failed to undergo G_1 arrest. Indeed, G_1 arrest measurements made at 12.6 Gy were more indicative of *p53* cDNA status that those made at 6.3 Gy. Our G_1 arrest results were obtained from irradiated cells that were incubated in medium containing the mitotic inhibitor nocodazole. Nocodazole was added to the assay to ensure that any cells that break through the G_2 checkpoint were prevented from reentering G_1 of the second cell cycle. Thus, the G_1 population that was measured 17 h following irradiation and incubation with nocodazole was composed of cells arrested in the first G_1 (20, 21).

Assessment of the γ-ray inducibility of mRNA transcribed from the *p53*-regulated genes *CIP1/WAF1*, *GADD45*, and *MDM2* revealed, in most cases, an apparent dependence upon wild-type *p53* sequence for strong induction of each transcript. Noteworthy exceptions included the curious lack of *GADD45* mRNA induction in some of the melanoma and renal cell lines, γ-ray induction of *CIP1/WAF1* mRNA in one mutant *p53* line, and *MDM2* mRNA induction in three mutant *p53* lines. Lack of induction of *GADD45* mRNA in some of the wild-type *p53* melanoma and renal lines contrasted with the strong induction of *CIP1/WAF1* mRNA in 5 of 6 lines. These results suggested that failure of p53 to induce *GADD45* mRNA resided at the level of the *GADD45* gene or mRNA stability. Sequencing of the third intron region of the *GADD45* gene, which contains the p53 binding element, revealed no sequence mutations in this region (37). A further investigation of these and other melanoma and renal cell lines will be necessary to explain this unexpected finding. The level of *MDM2* mRNA induction observed in the wild-type *p53* lines studied was relatively modest compared to that observed for either *CIP1/WAF1* or *GADD45* mRNA. Fifteen of the 18 wild-type *p53* lines tested exhibited induction of *MDM2* mRNA levels above 1.5-fold (Fig. 6). However, so did a number of mutant *p53* cell lines, including SF295, CCRFCEM, and HL60 cells. The basis for *MDM2* mRNA induction in these mutant *p53* lines requires further investigation, as does the finding of one mutant *p53* line, SNB75, that showed marked γ-ray inducibility of *CIP1/WAF1* mRNA. The latter result, however, was made relative to basal *CIP1/WAF1* mRNA levels, which in SNB75 cells were particularly low (data not shown).

Characterization of the integrity of the *p53* pathway in the NCI screen lines provided the opportunity to examine the activities of 123 standard agents for which putative action mechanisms had been assigned (5, 8, 10). Most of the clinically approved anticancer drugs were included within this set of compounds. Our goal here was to determine whether *p53* status was an important factor in the chemosensitivity of the 60 cell lines in the NCI screening assay. The results shown in Fig. 8 indicated that the majority of clinically active agents, including alkylating agents, antimetabolites, and topoisomerase I and II inhibitors, tended, in this assay system, to exhibit more growth suppression in the lines with normal *p53* status. This was the case whether the analysis was based on *p53* cDNA sequence or on most of the other factors that indicated an intact *p53* pathway. In contrast, cells with elevated p53 protein levels tended to be less sensitive to the majority of these same agents. This finding was consistent with the high frequency with which mutant *p53* gene status was observed in lines overexpressing p53 (Fig. 2).

Given the above findings, we have recently gone on to identify compounds for further investigation on the basis that their activity in this primary screen tended not to correlate with *p53* status or tended toward greater activity in the lines with mutant *p53* (Ref. 38 and data not shown). Although agents of the latter type were not uncovered among the 123 standard agents tested in the present report, a series of compounds that clearly differed from the majority of clinical drugs was the antitubulin series, which includes paclitaxel and vincristine. For these drugs, there was no correlation between *p53* status and chemosensitivity in the NCI screening assay. We uncovered similar findings in recent studies on a series of Burkitt's lymphoma cell lines and with a number of isogenic systems based on cancer cells with intact or disrupted *p53* function.[3] In contrast to the above findings,

[3] S. Fan, B. Cherney, and P. M. O'Connor. Disruption of p53 function in immortalized human cells does not affect survival or apoptosis following paclitaxel or vincristine treatment, submitted for publication.

however, it has been reported that *p53* disruption sensitizes normal fibroblasts to paclitacel (44). Although further studies are necessary, it is possible that the paclitaxel sensitization observed in normal cells lacking *p53* function may not always extend to cancer cell lines.

The differential cisplatin sensitivity of the wild-type and mutant *p53* lines in the NCI screen paralleled our earlier results in human lymphoma cells (21). In these previous studies, we correlated the reduced cisplatin sensitivity of the mutant *p53* lines with an evasion of *p53*-mediated apoptosis (21). Investigations into the susceptibility of the NCI cell screen lines to *p53*-dependent apoptosis might help extend our observations described in this report. We and others have found that disruption of *p53* function in breast cancer MCF-7 cells and some other cell lines can actually cause cisplatin sensitization (19, 25, 26). A major difference between MCF-7 cells and of those of lymphoid origin, however, is their susceptibility to *p53*-mediated apoptosis. In the case of lymphoid cells, activation of *p53* has been associated with apoptosis (21), whereas MCF-7 cells respond to *p53* activation by stably arresting in G_1 and G_2 (19). Cisplatin sensitization might be more clearly observed when cell types not inherently prone to *p53*-induced apoptosis have been disrupted for *p53* function. Given that the majority of the mutant *p53* lines in the NCI screen tended to be less sensitive to cisplatin than the wild-type *p53* lines, it seems that the responses of the NCI lines more closely resembled the responses observed in human lymphoma cells (21).[3] Further studies will be necessary to investigate whether apoptosis is an important determinant of the GI_{50}s recorded for the wild-type *p53* cell lines in the NCI cell screen.

The current NCI anticancer drug screen provides a short-term assay of chemosensitivity defined through growth inhibition. The assay screens approximately 10,000 compounds per year, and to date, over 60,000 agents have been tested against these lines. This assay cannot, with certainty, distinguish cytotoxicity from cytostasis, and agents selected from this primary screen based on interesting activity profiles against the lines therefore need to be tested in additional assays for cytotoxicity. Nonetheless, the results obtained in this short-term assay have already yielded useful insights into mechanisms of drug action, P-glycoprotein substrates, and agents preferentially active in cells with activated *ras* or nm23 expression differences (5, 8, 10–15, 32). In each case, agents and correlations have been discovered from these databases that might not have been found otherwise.

Our characterization of the *p53* tumor suppressor pathway in the NCI screen lines permitted the large database of compounds tested against these cell lines to be searched for agents that might have preferential activity against cells with defective *p53* function. The initial findings of these studies were briefly described in a recent report (38). Verification that any such lead compounds derived from this (38) or subsequent analyses actually behave differently in relation to *p53* status will clearly be necessary. This verification process will involve examination of compounds in isogenic systems consisting of parental wild-type *p53* lines and derivative cell types lacking *p53* function. This is possible through transfection with either a dominant-negative mutant *p53* gene or the human papillomavirus type-16 E6 gene (19, 26).[3] Other characteristics will have to be taken into account when appropriate cells for transfection are chosen. For example, cell types representative of the two contrasting arms of the *p53* response pathway, apoptosis and stable cell cycle arrest, will need to be tested in such studies. Longer-term assays of chemosensitivity, such as 6-day survival assays and clonogenic assays, as well as *in vivo* studies, are intended to confirm that lead compounds do indeed exhibit preferential cytotoxicity against cells with defective *p53* function.

The present report provides extensive information regarding the status of the *p53* pathway in cell lines of the NCI anticancer drug screen. This information should prove useful to researchers investigating fundamental aspects of *p53* biology and pharmacology. A summary of these findings and links to other molecular characteristics gathered on the NCI screen cell lines can be accessed through the World Wide Web at http://epnws1.ncifcrf.gov:2345/dis3d/dtp.html. This information on *p53* also enabled us to investigate the growth-inhibitory properties of a series of 123 standard agents previously characterized according to mechanism of drug action in the NCI screen. Our investigations revealed that cell lines with defective *p53* status tended, in this assay system, to be less sensitive to the majority of alkylating agents, antimetabolites, and topoisomerase I and II inhibitors. No such relationship was seen for the antimitotic agents, such as paclitaxel and vincristine. Our characterization of *p53* in these cell lines is enabling a large scale analysis of the more than 60,000 compounds tested in this primary screen. The next goal is to discover novel agents that act independently of *p53* function or that might exploit defective *p53* function as a means of preferential toxicity.

ACKNOWLEDGMENTS

We are grateful to Dr. Bert Vogelstein for the kind gift of the *WAF1* and *MDM2* cDNA probes and to members of the Developmental Therapeutics Program, NCI, for the chemosensitivity data used in this report. We are also grateful to Drs. Michael Grever and Bruce Chabner for their encouragement of the *p53* characterization of the NCI cell screen lines.

REFERENCES

1. Rubinstein, L. V., Shoemaker, R. H., Paull, K. D., Simon, R. M, Tosini, S., Skehan, P., Scudiero, D. A., Monks, A., and Boyd, M. R. Comparison of *in vitro* anticancer-drug-screening data generated with a tetrazolium assay *versus* a protein assay against a diverse panel of human tumor cell lines. J. Natl. Cancer Inst., *82:* 1113–1118, 1990.
2. Monks, A., Scudiero, D., Skehan, P., Shoemaker, R., Paull, K., Vistica, D., Hose, C., Langley, J., Cronise, P., Vaigro-Wolff, A., *et al.* Feasibility of a high-flux anticancer drug screen using a diverse panel of cultured human tumor cell lines. J. Natl. Cancer Inst., *83:* 757–766, 1991.
3. Grever, M. T., Schepartz, S. A., and Chabner, B. A. The National Cancer Institute Cancer Drug Discovery and Development Program. Semin. Oncol., *19:* 622–638, 1992.
4. Boyd, M. R., and Paull, K. D. Some practical considerations and applications of the National Cancer Institute *in vitro* anticancer drug discovery screen. Drug Dev. Res., *34:* 91–95, 1995.
5. Paull, K. D., Hamel, E., and Malspeis, L. Prediction of biochemical mechanism of action from the *in vitro* antitumor screen of the National Cancer Institute. *In:* W. O. Foye (ed.) Cancer Chemotherapeutic Agents, pp. 9–45. Washington, DC, American Chemical Society, 1995.
6. Paull, K. D., Lin, C. M., Malspeis, L., and Hamel, E. Identification of novel antimitotic agents acting at the tubulin level by computer-assisted evaluation of differential cytotoxicity data. Cancer Res., *52:* 3892–3900, 1992.
7. Cleaveland, E. S., Monks, A., Vaigro-Wolfe, A., Zaharevitz, D. W., Paull, K., Ardalan, K., Cooney, D. A., and Ford, H. J. Site of action of two novel pyrimidine biosynthesis inhibitors accurately predicted by the COMPARE program. Biochem. Pharmacol., *49:* 947–954, 1995.
8. Weinstein, J. N., Kohn, K. W., Grever, M. R., Viswanadhan, V. N., Rubinstein, L. V., Monks, A. P., Scudiero, D. A., Welch, L., Koutsoukos, A. D., Chiausa, A. J., and Paull, K. D. Neural computing in cancer drug development: predicting mechanism of action. Science (Washington DC), *258:* 447–51, 1992.
9. Myers, T. G., Anderson, N. L., Waltham, M., Li, G., Buolawini, J. K., Scudiero, D. A., Paull, K. D., Sausville, E. A., and Weinstein, J. N. A protein expression database for the molecular pharmacology of cancer. Electrophoresis, *18:* 647–653, 1997.
10. van Osdol, W. W., Myers, T. G., Paull, K. D., Kohn, K. W., and Weinstein, J. N. Use of the Kohonen self-organizing map to study the mechanisms of action of chemotherapeutic agents. J. Natl. Cancer Inst., *86:* 1853–1859, 1994.
11. Alvarez, M., Paull, K., Monks, A., Hose, C., Lee, J. S., Weinstein, J., Grever, M., Bates, S., and Fojo, T. Generation of a drug resistance profile by quantitation of mdr-1/P-glycoprotein in the cell lines of the National Cancer Institute Anticancer Drug Screen. J. Clin. Invest., *95:* 2205–2214, 1995.
12. Wu, L., Smythe, A. M., Stinson, S. F., Mullendore, L. A., Monks, A., Scudiero, D. A., Paull, K. D., Koutsoukos, A. D., Rubinstein, L. V., Boyd, M. R., and Shoemaker, R. H. Multidrug-resistant phenotype of disease-oriented panels of human tumor cell lines used for anticancer drug screening. Cancer Res., *52:* 3029–3034, 1992.
13. Lee, J. S., Paull, K., Alvarez, M., Hose, C., Monks, A., Grever, M., Fojo, A. T., and Bates, S. E. Rhodamine efflux patterns predict P-glycoprotein substrates in the National Cancer Institute drug screen. Mol. Pharmacol., *46:* 627–638, 1994.
14. Izquierdo, M. A., Shoemaker, R. H., Flens, M. J., Scheffer, G. L., Wu, L., Prather, T. R., and Scheper, R. J. Overlapping phenotypes of multidrug resistance among panels of human cancer-cell lines. Int. J. Cancer, *65:* 230–237, 1996.

15. Koo, H-M., Monks, A., Mikheev, A., Rubinstein, L. V., Gray-Goodrich, M., McWilliams, M. J., Alvord, W. G., Oie, H. K., Gazdar, A. F., Paull, K. D., Zarbl, H., and Vande Woude, G. F. Enhanced sensitivity to 1-β-D-arabinofuranosylcytosine and topoisomerase II inhibitors in tumor cell lines harboring activated ras oncogenes. Cancer Res., *56:* 5211–5216, 1996.
16. Hollstein, M., Sidransky, D., Vogelstein, B., and Harris, C. C. *p53* mutations in human cancers. Science (Washington DC), *253:* 49–52, 1991.
17. Levine, A., Momand, J., and Finlay, C. A. The *p53* tumor suppressor gene. Nature (Lond.), *351:* 453–456, 1991.
18. Hollstein, M., Shomer, B., Greenblatt, M., Soussi, T., Hovig, E., Montesano, R., and Harris, C. C. Somatic point mutations in the *p53* gene of human tumors and cell lines: updated compilation. Nucleic Acids Res., *24:* 141–146, 1996.
19. Fan, S., Smith, M. L., Rivet, D. J., II, Duba, D., Zhan, Q., Kohn, K. W., Fornace, A. J., Jr., and O'Connor, P. M. Disruption of *p53* function sensitizes breast cancer MCF-7 cells to cisplatin and pentoxifylline. Cancer Res., *55:* 1649–1654, 1995.
20. O'Connor, P. M., Jackman, J., Jondle, D., Bhatia, K., Magrath, I., and Kohn, K. W. Role of the *p53* tumor suppressor gene in cell cycle arrest and radiosensitivity of Burkitt's lymphoma cell lines. Cancer Res., *53:* 4776–4780, 1993.
21. Fan, S., El-Deiry, W. S., Bae, I., Freeman, J., Jondle, D., Bhatia, K. Fornace, A. J., Jr., Magrath, I., Kohn, K. W., and O'Connor, P. M. *p53* gene mutations are associated with decreased sensitivity of human lymphoma cells to DNA damaging agents. Cancer Res., *54:* 5824–5830, 1994.
22. Lowe, S. W., Ruley, H. E., Jacks, T., and Houseman, D. E. *p53*-dependent apoptosis modulates the cytotoxicity of anticancer agents. Cell, *74:* 957–967, 1993.
23. Lowe, S. W., Schmitt, E. M., Smith, S. W., Osborne, B. A., and Jacks, T. *p53* is required for radiation-induced apoptosis in mouse thymocytes. Nature (Lond.), *1362:* 847–849, 1993.
24. Slichenmyer, W. J., Nelson, W. G., Slebos, R. J., and Kastan, M. B. Loss of a *p53*-associated G_1 checkpoint does not decrease cell survival following DNA damage. Cancer Res., *53:* 4164–4168, 1993.
25. Hawkins, D. D., Demers, G. W., and Galloway, D. A. Inactivation of *p53* enhances sensitivity to multiple chemotherapeutic agents. Cancer Res., *56:* 892–898, 1996.
26. Fan, S., Chang, J., Smith, M. L., Duba, D., Fornace, A. J., Jr., O'Connor, P. M. Cells lacking CIP1/WAF1 genes exhibit preferential sensitivity to cisplatin and nitrogen mustard. Oncogene, *14:* 2127–2136, 1997.
27. Vasey, P. A., Jones, N. A., Jenkins, S., Dive, C., and Brown, R. Cisplatin, camptothecin and paclitaxel sensitivities of cells with *p53*-associated multidrug resistance. Molecular Pharmacology, *50:* 1536–1540, 1996.
28. Ishioka, C., Frebourg, T., Yan, Y. X., Vidal, M., Friend, S. H. Schmidt, S., and Iggo, R. Screening patients for heterozygous *p53* mutations using a functional assay in yeast. Nat. Genet., *5:* 124–129, 1993.
29. Kern, S. E., Kinzler, K. W., Bruskin, A., Jarosz, D., Friedman, P., Prives, C., Vogelstein, B. Identification of *p53* as a sequence-specific DNA-binding protein. Science (Washington DC), *252:* 1708–1711, 1991.
30. Jackman, J., Alamo, I., Jr., and Fornace, A. J., Jr. Genotoxic stress confers preferential and coordinate messenger RNA stability on the five GADD genes. Cancer Res., *54:* 5656–5662, 1994.
31. Hollander, M. C., and Fornace, A. J., Jr. Induction of fos RNA by DNA-damaging agents. Cancer Res., *49:* 1687–1692, 1989.
32. Freije, J. M. P., Lawrence J. A., Hollingshead, M. G., De La Rosa, A., Narayanan. V., Grever, M., Sausville, E. A., Paull, K., and Steeg, P. S. Identification of compounds with preferential inhibitory activity against low-Nm23-expressing human breast carcinoma and melanoma cell lines. Nature Medicine, *3:* 395–401, 1997.
33. Greenblatt, M. S., Bennett, W. P., Hollstein, M., and Harris, C. C. Mutations in the *p53* tumor suppressor gene: clues to cancer etiology and molecular pathogenesis. Cancer Res., *54:* 4855–4878, 1994.
34. Jayaraman, J., and Prives, C. Activation of *p53* sequence-specific DNA binding by short single strands of DNA requires the *p53* C-terminus. Cell *81:* 1021–1029, 1995.
35. Lee, S., Elenbaas, B., Levine, A., and Griffith, J. *p53* and its 14 kDa C-terminal domain recognize primary DNA damage in the form of insertion/deletion mismatches. Cell, *81:* 1013–1020, 1995.
36. Kastan, M. B., Onyekwere, O., Sidransky, D., Vogelstein, B., and Craig, R. W. Participation of *p53* protein in the cellular response to DNA damage. Cancer Res., *51:* 6304–6311, 1991.
37. Bae, I., Smith, M. L., Sheikh, M. S., Zhan, Q., Scudiero, D. A., Friend, S. H., O'Connor, P. M., and Fornace, A. J., Jr. An abnormality in the *p53* pathway following gamma irradiation in many wild-type *p53* human melanoma lines. Cancer Res., *56:* 840–847, 1996.
38. Weinstein, J. N., Myers, T. G., O'Connor, P. M., Friend, S. H., Fornace, A. J., Kohn, K. W., Fojo, T., Bates, S. E., Rubinstein, L. V., Anderson, N. L., Buolamwini, J. K., van Osdol, W. W., Monks, A. P., Scudiero, D. A., Sausville, E. A., Zaharevitz, D. W., Bunow, B., Viswanadhan, V. N., Johnson, G. S., Wittes, R. E., and Paull, K. D. An information-intensive approach to the molecular pharmacology of cancer. Science (Washington DC), *275:* 343–349, 1997.
39. Bhatia, K., Goldschmidts, W., Gutierrez, M., Gaidano, G., Dalla-Favera, R., and Magrath, I. Hemi- or homozygosity: a requirement for some but not other *p53* mutant proteins to accumulate and exert a pathogenetic effect. FASEB J., *7:* 951–956, 1993.
40. Brachman, D. G., Beckett, M., Graves, D., Haraf, D., Vokes, E., and Weichselbaum, R. R. *p53* mutation does not correlate with radiosensitivity in 24 head and neck cancer cell lines. Cancer Res., *53:* 3667–3669, 1993.
41. Kern, S. E., Redston, M., Seymour, A. B., Caldas, C., Powell, S. M., Kornacki, S., and Kinzler, K. W. Molecular genetic profiles of colitis-associated neoplasms. Gastroenterology, *107:* 420–428, 1994.
42. Winter, S. F., Minna, J. D., Johnson, B. E., Takahashi, T., Gazdar, A. F., and Carbone, D. P. Development of antibodies against *p53* in lung cancer patients appears to be dependent on the type of *p53* mutation. Cancer Res., *52:* 4168–4174, 1992.
43. Cho, Y., Gorina, S., Jeffrey, P. D., and Pavletich, N. P. Crystal structure of a *p53* tumor suppressor-DNA complex: understanding tumorigenic mutations. Science (Washington DC), *265:* 346–356, 1994.
44. Wahl, A. F., Donaldson, K. L., Fairchild, C., Lee, F. Y., Foster, S. A., Demers, G. W., and Galloway, D. A. Loss of normal *p53* function confers sensitization to paclitaxel by increasing G_2-M arrest and apoptosis. Nat. Med., *2:* 72–79, 1996.